universität wien

MASTERARBEIT

Titel der Masterarbeit

„Atherogenic effects of lipoprotein carbamylation, uremia and hemodialysis in macrophages“

Verfasserin

Marianne Hollaus, BSc

angestrebter akademischer Grad

Master of Science (MSc)

Wien, 2012

Studienkennzahl lt. Studienblatt:	A 066 834
Studienrichtung lt. Studienblatt:	Masterstudium Molekulare Biologie
Betreuer:	o. Univ.-Prof. Dr. Wolfgang Schneider

Danksagung

Ich möchte mich bei all jenen bedanken, die zur Realisierung dieser Arbeit beigetragen haben.

Mein größter Dank gilt meiner Betreuerin Monika Strobl, die mir meine Masterarbeit am Institut für Medizinische Chemie ermöglicht hat. Danke liebe Monika, für deine Führung und Unterstützung und für die Beantwortung meiner zahlreichen Fragen.

Sabine Meier hat mich von Beginn an kompetent unterstützt und durch sie konnte ich mir sehr viel Laborwissen aneignen. Sabine, ich bin dir sehr dankbar dafür, dass du mir jederzeit hilfsbereit zur Seite gestanden bist - nicht nur beruflich, sondern auch in privaten Dingen.

Herbert Stangl möchte ich für seine fachliche Hilfe sowie für seine positive Zusprache danken. Seine motivierenden Worte lenkten meinen Blick oft wieder nach vorne.

Bei Clemens Röhrl, Stefanie Fruhwürth, Katharina Winter, Lisa Pemberger, Markus Amman und Jelena Brankovic bedanke ich mich für die hervorragende und hilfsbereite Zusammenarbeit sowie für den Spaß im Labor. Ich danke euch auch für das tolle Arbeitsklima und es war schön mit euch so oft zu lachen.

Ich werde die gemeinsame Zeit missen, vor allem die Diskussionen und Gespräche beim Mittag- und Kuchenessen.

Vielen weiteren Mitarbeitern des Instituts möchte ich für die freundliche Atmosphäre und den netten Umgang danken.

Ein großer Dank gilt auch meiner Mutter und meiner Familie, meinen Freunden sowie meinem Partner Christoph. Sie alle haben mich persönlich unterstützt und sind immer hinter mir gestanden.

Table of Contents

1 Indices

1.1 Index of tables

1.2 Index of figures

1.3 List of abbreviations

ABC	ATP-binding cassette
ABCA1	ATP-binding cassette transporter A1
ABCG1	ATP-binding cassette transporter G1
acLDL	acetylated LDL
ANOVA	analysis of variance
APS	ammonium persulfate
ATCC	american type culture collection
ATP	adenosine triphosphate
BSA	bovine serum albumin
CAC	cholesterol acceptor capacity
CD36	cluster of differentiation 36
cDNA	complementary DNA
cHDL	carbamylated HDL
cLDL	carbamylated LDL
CRF	chronic renal failure
CT	treshhold cycle
DNA	deoxyribonucleic acid
dpm	disintegrations per minute
EDTA	ethylenediamine tetraacetic acid
EGTA	ethylene glycol tetraacetic acid
ESRD	end-stage renal disease
FCS	fetal calf serum
GGPP	geranyl-geranyl-pyrophosphate
Hcit	homocitrulline
HDL	high density lipoprotein
HMDM	human monocyte-derived macrophages
HMG-CoA	3-hydroxy-3-methyl-glutaryl-coenzyme A
KBr	potassium bromide
KCNO	potassium cyanate
KDOQI	kidney disease outcomes quality initiative
LCAT	lecitin-cholesterol acyltransferase
LDL	low density lipoprotein
LOX-1	lectin-type oxidized LDL receptor 1
LXR	liver X receptor
M-CSF	macrophage-colony stimulating factor
miR	see miRNA
miRNA	microRNA
mRNA	messenger RNA
NaOH	sodium hydroxide
nHDL	native HDL
nLDL	native LDL
NR1H3	nuclear receptor subfamily 1, group H, member 3; LXRα
oxLDL	oxidized LDL
PBMC	peripheral blood mononuclear cells
PBS	phosphate buffered saline
PCR	polymerase chain reaction
PMA	phorbol 12-myristate 13-acetate
qPCR	quantitative real-time PCR

RCT	reverse cholesterol transport
REM	relative electrophoretic mobility
RNA	ribonucleic acid
RPMI	Rosswell Park Memorial Institute
RQ	relative quantitation
rRNA	ribosomal RNA
RXR	retinoid X receptor
SCARB1	see SR-BI
SD	standard deviation
SDS	sodium dodecyl sulfate
SDS-PAGE	sodium dodecyl sulfate polyacrylamide gel electrophoresis
SMC	smooth muscle cell
SR-A	scavenger receptor class A
SR-BI	scavenger receptor class B type I
SREBP	sterol regulatory element binding protein
TAE	tris-acetate EDTA
TBS	tris buffered saline
TBS-T	TBS-Tween
TEMED	tetramethylethylenediamine
UDG	uracil-DNA glycosylase
UTR	untranslated region
VLDL	very low density lipoprotein

2 Introduction

According to the Global Burden of Disease analysis of the World Health Organization, cardiovascular diseases are the most common causes of death in industrialized societies (World Health Organization, 2008). Among this class of diseases, atherosclerosis is characterized by the formation of atheromatous plaques in the arterial wall that further may lead to medical complications such as myocardial infarction or stroke (Glass et al., 2001; Libby et al., 2011). Atherosclerosis has been subject to intense investigation but its pathomechanisms are not yet fully understood. Atherosclerosis is a multifactorial disease and both, genetic and environmental influences, like smoking or a high-fat and cholesterol diet, contribute to the risk for this disease (Glass et al., 2001; Moore et al., 2011).

2.1 Development of atherosclerosis

In general, atherogenesis occurs in several stages as schematized in figure 1. Inflammation at sites of the arterial wall contributes to the initiation of the development of lesions or plaques within the vascular lumen (Ross, 1999). This narrows the arteries and further reduces their flexibility, which in turn leads to a reduced supply with oxygen-rich blood to vital organs (Watkins et al., 2006). Acute clinical complications come up when plaque formation consistently continues, as the risk of a plaque rupture increases. Formation of a thrombus raises the danger for myocardial infarction or stroke (Libby et al., 2011).

Disturbed laminar flow in arteries, which often occurs at arterial branch sites, predominantly facilitates atherosclerotic progression as shear stresses of blood flow decrease and turbulences increase (Ross, 1999; Moore et al., 2011).

The accumulation of apolipoprotein B-containing lipoproteins (such as low-density lipoprotein, LDL) in the subendothelial space results in endothelial dysfunction and together with inflammation, these events represent the initial step (figure 1A) in atherosclerosis (Ross, 1999). Overlying endothelial cells secrete chemokines and thereby recruit monocytes and T lymphocytes, express adhesion molecules and increase their permeability in response to inflammatory stimuli (Glass et al., 2001).

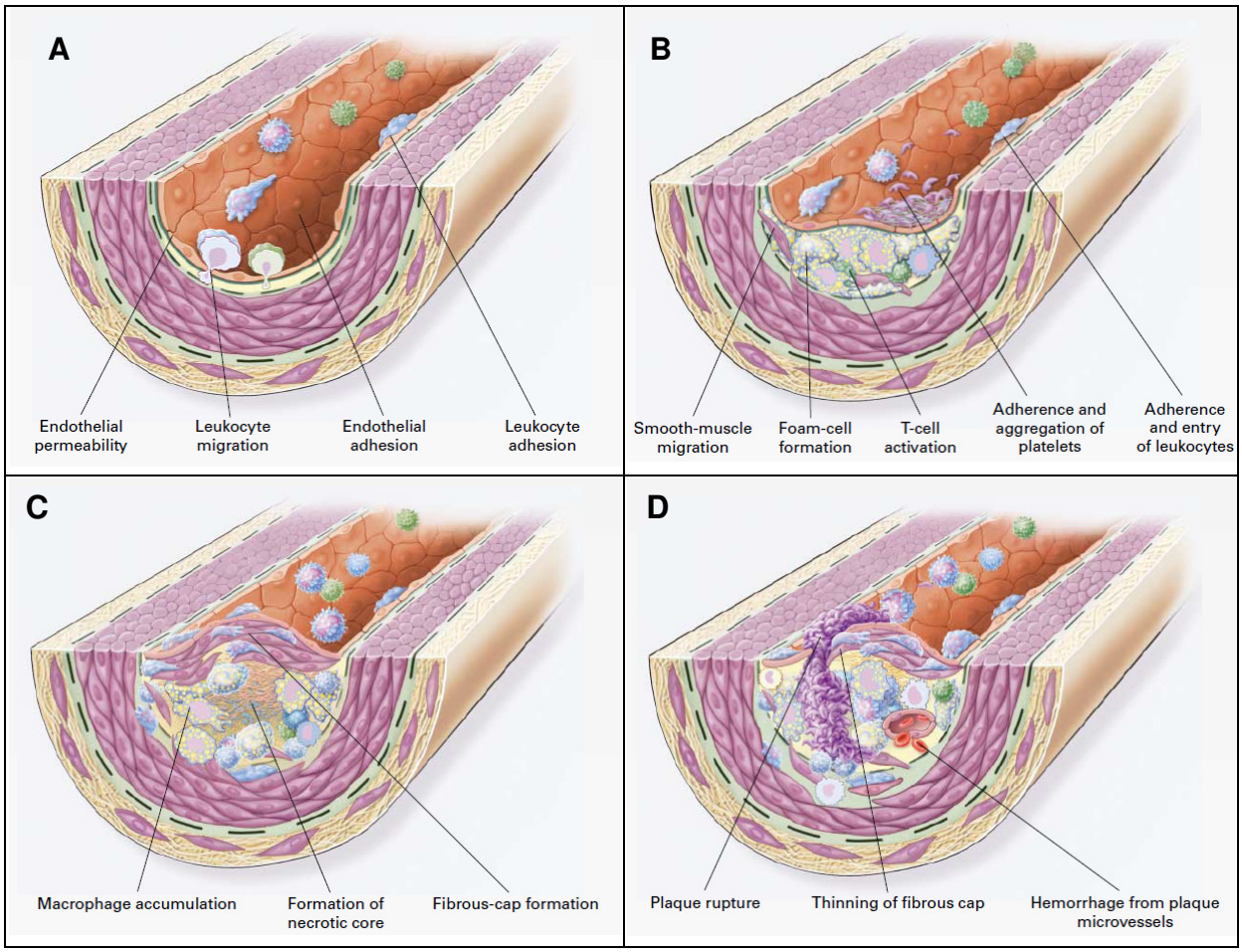

Figure 1: Stages of atherosclerosis
Endothelial dysfunction (A); Formation of the fatty streak (B); advanced complicated lesion formation (C); unstable fibrous plaque (D). Figures adapted from Ross, 1999

Adhesion of monocytes to the endothelium allows their entry in the subendothelial space and thereafter, macrophage-colony stimulating factor (M-CSF) effects their differentiation into macrophages. Macrophages acquire several functions during differentiation. The expression of scavenger receptors and toll-like receptors is upregulated and thus, the ability of macrophages to internalize apoptotic cell fragments and modified LDL particles is increased (reviewed by Pello et al., 2011). However, little is known about the regulation of the cholesterol efflux transporters during macrophage differentiation.

Modified forms of LDL are taken up by intimal macrophages and this process leads to the formation of so called foam cells. Foam cells are characterized by massive intracellular accumulation of cholesteryl esters and they are the main component of the fatty streak (figure 1B) and hence, they are characteristic for early atherosclerotic lesions (Libby et al., 2011). With further progression of atherosclerosis, smooth muscle

cells (SMCs) and T-cells migrate to the intima and leukocytes invade the subendothelial space. SMCs in the intima produce extracellular matrix proteins, which increase the volume of the lesion. A fibrous cap, which covers the atheromata is formed (figure 1C). The cap represents a boundary between lesion and lumen and may be considered to be a response to the injury of the endothelium (Ross, 1999). However, with atherosclerosis progression, monocytes continue to immigrate into the intima. Due to prolonged endoplasmic reticulum stress and other stimuli, macrophages undergo apoptosis (Moore et al., 2011). A necrotic core (figure 1C) develops as result of apoptosis of lesional macrophages and their ineffective phagocytosis. The necrotic core contributes to physical stress on the fibrous cap and may initiate thrombus formation since it contributes to further inflammation. The fibrous cap undergoes changes due to macrophage-derived matrix metalloproteinases, which degrade the extracellular matrix and other proteolytic enzymes (Moore et al., 2011). Thus, the fibrous cap becomes instable, which in turn increases the probability of a rupture (figure 1D). When the plaque ruptures, plaque material gets exposed to the lumen. Consequently, the coagulation cascade is initiated, platelets aggregate at the rupture site and a thrombus forms (for reviews see Ross, 1999; Glass et al., 2001; Libby et al., 2011; Moore et al., 2011).

2.2 Cholesterol metabolism

Cholesterol is an important component of animal cells which plays many roles, among them providing rigidity to cell membranes, serving as precursor molecule for steroid hormones or bile acids (Maxfield et al., 2010) and as a component of signaling pathways (Incardona et al., 2000). Cholesterol metabolism is tightly regulated and dysregulation of cholesterol homeostasis is associated with diseases such as atherosclerosis (Glass et al., 2001).

The synthesis of cholesterol proceeds from acetyl-CoA through many enzymatic reactions (Sato et al., 1995) with HMG-CoA (hydroxymethylglutaryl-Coenzyme A) reductase as rate limiting enzyme. Since this process is very energy consuming, cells retrieve cholesterol from the circulation by uptake of LDL via the LDL-receptor, which is located on the plasma membrane (Goldstein et al., 1977). Tight control of the intracellular cholesterol level is a prerequisite for maintaining cholesterol homeostasis. When the intracellular cholesterol concentration is low, sterol regulatory element

binding-proteins (SREBP) are activated, move from the cytosol to the nucleus and initiate transcription of genes responsible for cholesterol synthesis (HMG-CoA reductase) and uptake (LDL-receptor). In case of a cholesterol excess within the cell, HMG-CoA reductase activity is reduced and LDL-receptor expression declines (Goldstein et al., 2006). Furthermore, oxysterols are produced which bind to LXR (liver x receptor), thereby initiating heterodimerization of LXR with RXR (retinoid x receptor). This LXR/RXR complex activates expression of genes involved in cholesterol efflux (Tall, 2008).

2.3 Reverse cholesterol transport and cholesterol efflux from macrophages

The process of returning cholesterol from the periphery to the liver for excretion is known as reverse cholesterol transport (RCT). As described above (cpt. 2.2), cells retrieve cholesterol through the uptake of lipoproteins or *de novo* synthesis and cellular cholesterol homeostasis is strictly regulated. Peripheral cells, including vascular macrophages, are unable to degrade excess free cholesterol, which is toxic for them. Therefore, the mechanism used to avoid accumulation of surplus free cholesterol within cells is RCT (Francis et al., 1999).

High density lipoprotein (HDL) is the key molecule in RCT and hence, it makes an important contribution to atheroprotection. The process of reverse cholesterol transport from macrophages is dependent on adenosine triphosphate (ATP) binding cassette transporters, mainly ABCA1 and ABCG1 (Tall, 2008). Efflux of cholesterol and phospholipids from macrophages to lipid poor apoA-I, which represents nacent HDL, occurs via ABCA1 on the cell membrane, while mature HDL requires attachment to ABCG1 to accept cholesterol (Yvan-Charvet et al., 2009). Furthermore, ABCA1-mediated cholesterol efflux initiates the maturation of HDL by addition of lipids to apoA-I and hence, ABCA1 and ABCG1 act synergistically, with ABCA1 generating nascent HDL particles which then further may serve as substrates for cholesterol efflux via ABCG1 (Gelissen et al., 2006). The enzyme lecitin-cholesterol acyltransferase (LCAT) is bound to the surface of HDL and is responsible for esterification of free cholesterol. Cholesterol esters are more hydrophobic than free cholesterol and therefore, cholesterol esters are transferred to the core of the HDL particle (Fielding et al., 1995). After loading, HDL travels via the blood stream to the liver where it binds preferably to

the scavenger receptor class B type I (SR-BI) for release of cholesterol and phospholipids (Valacchi et al., 2011).

Besides ABCA1 and ABCG1, other molecules are also involved in cholesterol efflux from macrophages. One of them is SR-BI, which is an ubiquitous receptor and hence, also present on macrophages. There, it contributes to the efflux of free cholesterol from macrophages. SR-BI, however, is a bidirectional transporter and can also promote uptake of cholesterol and therefore its importance in macrophage RCT remains questionable (Valacchi et al., 2011; Cuchel et al., 2006).

The main cause for foam cell formation is an imbalance between cholesterol efflux and extensive uptake of modified LDLs (Rader et al., 2005; Moore et al., 2006) as described in the next chapter. The mechanism of macrophage RCT is not efficient enough to compensate for this excessive cholesterol uptake.

2.4 Modification of Low-Density Lipoproteins

LDL is a macromolecule, consisting of phospholipids, cholesteryl ester, free cholesterol, triglycerides and apolipoprotein apoB-100 and it is taken up by specific LDL receptors on cells (Goldstein et al., 1977). Many of the components of LDL are prone to modification, which alters the affinity for the LDL receptor. Modified LDLs are taken up nonspecifically by scavenger receptors. In contrast to the LDL-receptor, which is downregulated when increased amounts of intracellular cholesterol are present, scavenger receptor uptake occurs in a nonspecific and unregulated manner and huge amounts of lipids are ingested by macrophages as they keep taking up modified LDL (Itabe, 2003).

The present study involves three different modifications on the LDL particle: oxidation, carbamylation and acetylation. Besides oxidation and carbamylation, which are *in vivo* relevant modifications, and therefore explained in detail below, acetylation of LDL has not been described as physiological modification of LDL in the human body (Itabe, 2003). However, acLDL is often used *in vitro* in macrophage and endothelial cell models to initiate stable foam cell formation since it is extensively taken up by cells via several scavenger receptors (Goldstein et al., 1979; Kunjathoor et al., 2002). Thus, this modification *per se* has no relevance for atherosclerosis, but it allows the study of cholesterol loaded foam cells.

2.4.1 Oxidized LDL

Generally, LDL is protected from oxidation in plasma, but when it is localized in the subendothelial space, it is prone to oxidation by both, enzymatic and nonenzymatic modifications (Glass et al., 2001). The lipid components as well as the amino acids of apoB-100 are susceptible to oxidative modification and the properties of oxidized LDL depend on the extent of oxidation. While an early form of oxidized LDL, often referred to as minimally oxidized LDL, is still recognized by the LDL-receptor (Navab et al., 1996), higher oxidized forms of LDL (oxLDL) are taken up by macrophages and smooth muscle cells nonspecifically by scavenger receptors (Glass et al., 2001). OxLDL contains a fragmented apoB particle, in which lysine residues are covalently modified with reactive breakdown products of oxidized lipids (Glass et al., 2001). Thus, the LDL-receptor is not able to recognize oxLDL and its nonspecific uptake via scavenger receptors on macrophages leads to foam cell formation (Steinberg et al., 2010). Many scavenger receptors, which mediate the uptake of oxLDL have been described. Among them are CD36, LOX-1 (lectin-type oxidized LDL receptor 1) or SR-A (scavenger receptor A). SR-BI may also be a ligand for oxLDL (Goyal et al., 2012). In addition, interaction of oxLDL with macrophages leads to many proinflammatory and proatherogenic effects such as induction of cellular and humoral immune responses, increased apoptosis and necrosis, increased monocyte adhesion to endothelial cells and production of chemokines. These effects may be induced by oxLDL binding to scavenger receptors and activation of signal transduction cascades (Moore et al., 2006; Miller et al., 2009).

2.4.2 Carbamylated LDL

Carbamylation is a posttranslational modification of proteins without involvement of enzymes (Jaisson et al., 2011). Structure and functionality of proteins is altered when they are carbamylated due to an irreversible reaction of isocyanic acid with amino groups and N-terminal groups of amino acids in apoB-100, the main protein component of LDL, as schematized in figure 2 (Apostolov et al., 2012).

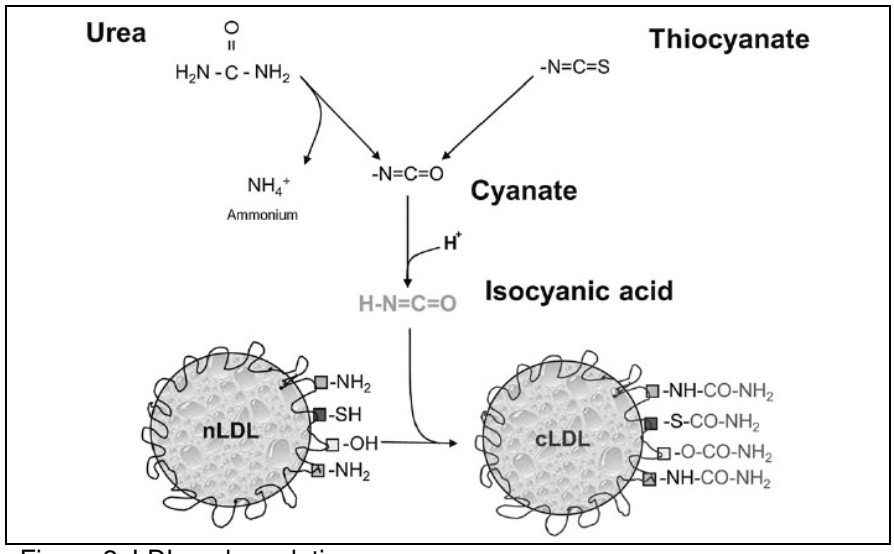

Figure 2: LDL carbamylation
Figure adapted from Apostolov et al., 2012

Two forms of isocyanic acid formation have been described (figure 2). First, urea spontaneously decomposes into cyanate and ammonia, thereafter cyanate is immediately converted into isocyanic acid (Jaisson et al., 2011). Another mechanism for isocyanic acid formation occurs via the metabolism of thiocyanate, which is an abundant anion in blood. Here, cyanate originates from an myeloperoxidase-catalyzed oxidation of thiocyanate under consumption of hydrogen peroxide (Wang et al., 2007b). Isocyanic acid is highly reactive with amino groups of proteins and therefore responsible for their carbamylation (Jaisson et al., 2011).

Carbamylated LDL (cLDL) has several pro-atherogenic effects such as contribution to foam cell formation, induction of endothelial cell apoptosis and smooth muscle cell proliferation (Ok et al., 2005; Wang et al., 2007b). As compared to native LDL (nLDL), the uptake of cLDL via the LDL-receptor is diminished. As a consequence, cLDL is cleared from the circulation slower than nLDL *in vivo* (Hörkkö et al., 1994) and thus may undergo additional modification via oxidation. Furthermore, cLDL is recognized by macrophage scavenger receptors, presumably SR-A1 (Wang et al., 2007b), and this in turn leads to nonspecific uptake of cLDL and induction of unspecific signaling pathways. Patients with chronic renal failure have an increased risk for atherosclerosis which may, besides other factors, be due to increased plasma urea levels, resulting in enhanced carbamylation of (lipo)proteins (Apostolov et al., 2010).

It is unclear, however, whether macrophages compensate for the increased nonspecific uptake of cLDL or whether cellular cholesterol efflux is even unpaired in

uremia (Zuo et al., 2009). Thus the present study tries to answer this question by investigating cLDL-induced changes in macrophage cholesterol efflux and in the expression of the transporters mediating this efflux process.

2.5 MicroRNAs and atherosclerosis

MicroRNAs (miRNAs, miRs) are highly conserved, noncoding, single stranded RNA molecules with a length of ~22 nucleotides in their mature form (Ambros, 2004). They are transcribed from intronic or exonic regions of protein coding genes or intergenic regions and after multiple processing steps, mature miRNAs exert their actions post-transcriptionally on the messenger RNAs (mRNAs) of proteins (Moore et al., 2010). Therefore, miRNAs bind preferably to the 3' untranslated region (UTR) by imperfect base paring and this causes translational repression or degradation of the target mRNA (Chekulaeva et al., 2009).

Although the contribution of miRNAs to several diseases, such as cancer, has been studied intensively (Ha, 2011b; Ha, 2011a), their role in the pathogenesis of atherosclerosis is not well defined and studies thereof are rare. MiRNAs have also been shown to have an impact on cholesterol homeostasis, and therefore may play a role in the development of atherosclerosis (Moore et al., 2010).

Recent studies showed, that miR-33a downregulates the expression of ABCA1 and ABCG1, and hence, plays a role in the regulation of cholesterol efflux. Furthermore, it has been reported that intronic regions of the gene encoding SREBP2 include the locus of miR-33a and thus, both possibly play in concert in the regulation of the cholesterol homeostasis (Rayner et al., 2010). Another regulator of cholesterol homeostasis may be miR-223 which targets the mRNA of SR-BI. Moreover, miR-223 is significantly increased in mouse models of atherosclerosis as well as in patients with familial hypercholesterolemia (Vickers et al., 2011).

Based on this information, we investigated the influence of modified LDLs on miR-33a and miR-223 expression in macrophages to determine a potential role of these miRNAs in the regulation of ABCA1, ABCG1 and SR-BI.

2.6 Chronic renal failure and atherosclerosis

Accelerated atherosclerosis is often found in patients with chronic renal failure (CRF). The increased risk for atherosclerosis in these patients is thought to be triggered primarily by oxidative stress, inflammation and dyslipidemia (Vaziri et al., 2011). CRF leads to reduced serum apoA-I and HDL cholesterol concentrations and to impaired HDL maturation (Vaziri et al., 2011). Reduced HDL cholesterol and impaired HDL maturation is associated with LCAT deficiency as result of renal insufficiency (Moradi et al., 2009b). In addition, the composition of HDL in patients with CRF is altered and its antioxidant activity is reduced (Moradi et al., 2009a). Increased oxidative stress in CRF leads to oxidation of molecules such as LDL (Himmelfarb et al., 2002) which in turn are taken up by macrophages of the arterial wall, and as consequence, foam cell formation is initiated. Since HDL composition in CRF-patients is altered, its reverse cholesterol transport capacity may be reduced (Vaziri et al., 2011).

Moreover, elevated plasma urea levels in patients with CRF induce the LDL carbamylation (Jaisson et al., 2011) which is known to be an atherogenic factor (Apostolov et al., 2010) as described in cpt. 2.4.2. Besides LDL, also HDL may undergo carbamylation. However, the carbamylation of HDL has not been studied as intensively as that of LDL. Carbamylated HDL (cHDL) has been reported to contribute to foam cell formation in tissue culture and it was found in atherosclerotic lesions in high concentrations (Holzer et al., 2011). We studied the cholesterol efflux capacity of cHDL and of serum from patients with either CRF or end stage renal disease (ESRD) on hemodialysis treatment.

3 Aim

Foam cells are the main component of the fatty streak and they are characteristic for early atherosclerotic lesions. Due to the extensive uptake of modified lipoproteins, foam cells contain massive amounts of cholesteryl esters (Libby et al., 2011). Carbamylation of LDL is increased in patients with CRF as result of uremia. The uptake of cLDL by macrophages induces foam cell formation and therefore is considered as atherogeneic (Jaisson et al., 2011).

So far, most studies have investigated the effects of cLDL in endothelial cells but little is known about its effect on (human) macrophages. Therefore, our first aim was to determine whether cLDL alters the expression of the efflux transporters ABCA1 and ABCG1 on a protein and mRNA level in THP-1 macrophages as response to excessive cholesterol uptake. The bidirectional receptor SR-BI may also play a role in the efflux of cholesterol (Valacchi et al., 2011). Therefore, we also examined the effect of cLDL on SR-BI protein and mRNA expression. Moreover, cholesterol efflux from THP-1 macrophages incubated with cLDL and nLDL to apoA-I, HDL and serum was measured to find any possible alterations. Since the transcription factor LXRα regulates ABCA1 and ABCG1 expression (Tall, 2008), it was of interest whether cLDL induces a change in LXRα mRNA expression, and in addition, it was tested whether antagonizing LXR reverses any possible effect.

Another aim was to characterize the mRNA and protein expression of ABCA1, ABCG1, SR-BI and LXRα during THP-1 differentiation from the monocytic state to macrophages. The gene expression of ABCA1, ABCG1 (reviewed by Tall, 2008) and SR-BI (Malerod et al., 2002; Hu et al., 2010) is regulated by LXRα in differentiated macrophages. We asked, whether the expression of this set of genes correlates with that of LXRα during THP-1 differentiation as well.

Furthermore, we aimed to investigate whether the expression of two specific miRNAs, namely miR-33a and miR-223, is altered when THP-1 macrophages are treated with different forms of modified LDLs. Both miRNAs are supposed to play a role in cholesterol homeostasis: miR-33a inhibits the expression of ABCA1 (Rayner et al., 2010) and miR-223 may target SR-BI for its degradation or repression (Vickers et al., 2011).

Finally, we studied the cholesterol acceptor capacity of carbamylated HDL to determine whether this modification impairs the acceptor capacity of HDL. Like LDL and other proteins, HDL is subject to carbamylation under uremic conditions (Wang et al., 2007b). In this context, we also measured the cholesterol acceptor capacity of serum obtained from patients with CRF or ESRD on hemodialysis treatment.

4 Materials and Methods

Chemicals used throughout the experiments were purchased from Merck (E.Merck, Darmstadt, Germany); Roth (Carl Roth GmbH, Karlsruhe, Germany) or Sigma (Sigma-Aldrich, St. Louis, USA) unless noted otherwise.

4.1 Cell culture

Two different cell models were used: The human monocytic cell line THP-1 (ATCC TIB-202) was used in most experiments. Primary human monocyte derived macrophages (HMDM), were used as a second cell model to confirm several results obtained with THP-1 cells.

4.1.1 THP-1 cells

THP-1 is a leukemia cell line which was derived from the peripheral blood of a one year old infant with acute moncytic leukemia (Tsuchiya et al., 1980). Incubation of these cells with phorbol esters induces their differentiation into macrophages (Tsuchiya et al., 1982).

Monocytic THP-1 cells were cultured in cell culture flasks (Greiner Bio One, Kremsmünster, Austria) at 37 °C under 5 % CO_2 atmosphere in RPMI-1640 medium (Rosswell Park Memorial Institute) supplemented with 2 mM L-glutamine, 0.1 mg/ml streptomycin, 100 U/ml penicillin (PAA, Pasching, Austria) and 10 % fetal calf serum (heat inactivated FCS, Gibco, Life Technologies Corporation, Carlsbad, USA). Cell number and viability were measured using a CASY® Cell Counter + Analyser System Model TT (Schärfe Systeme, Reuttlingen, Germany) and every two to three days, the cells were fed with fresh medium to a density of $0.7*10^6$ cells/ml.

To differentiate THP-1 cells from monocytes (suspension cells) towards adherent macrophages, $0.5*10^6$ cells/ml were incubated with 160 nM PMA (phorbol 12-myristate 13-acetate) for 72 hours. Therefore, the cells were seeded in multiwell plates (Greiner Bio One, Kremsmünster, Austria), provided that the viability was greater than 95 %, as measured with the CASY system. Seeding of cells occurred under the conditions as described in table 1:

Well format	Growth area per well (cm^2)	Volume per well (ml)
6 well plate	9.6	3
12 well plate	3.9	1.2
24 well plate	1.9	0.6

Table 1: Seeding of THP-1 cells in multiwell plates

4.1.2 Human monocyte derived macrophages

For isolation of peripheral blood mononuclear cells (PBMC), venous blood of adult fasting healthy volunteers was collected using a Vacuette® blood collection set, Vacuette® EDTA (EDTA, ethylene diamine tetra-acetic acid) tubes and Vacuette® serum tubes (Greiner Bio One, Kremsmünster, Austria). Isolation of mononuclear cells was performed using Ficoll-Paque™ PREMIUM (GE Healthcare, Buckinghamshire, UK), according to the manufacturer's instructions. The entire procedure was carried out under sterile conditions.

EDTA-tubes were centrifuged at 620 x g for 10 minutes at 18 °C without brake. Plasma was removed carefully, leaving the lymphocyte interphase intact and replaced by an identical volume of RPMI-1640. Blood and RPMI-1640 were gently mixed. Plasma was stored at 4 °C for lipoprotein preparation (see next section). Serum tubes were centrifuged at 1500 x g for 10 minutes at 18 °C and the upper serum layer was transferred to a new tube. An aliquot of serum was removed and stored at 4 °C until use on the same day. From the remaining serum, aliquots were prepared and stored at -20 °C.

Next, a tube containing Ficoll-Paque™ PREMIUM was prepared and an equal volume of the blood/RPMI-sample was layered over the Ficoll-Paque solution without allowing both phases to mix. Then, the samples were centrifuged at 320 x g for 30 minutes at 18 °C without brake. After centrifugation, four distinct layers were distinguishable. The uppermost layer contained medium, remaining plasma and platelets. The second layer was a white ring of PBMC. Beneath this ring, a layer containing Ficoll-Paque solution was present and the bottom layer was composed of erythrocytes and granulocytes.

The uppermost layer was drawn off and the PBMC ring was collected into a tube with fresh media for washing. Therefore, the cell isolate was suspended gently in 30 ml media and afterwards centrifuged at 320 x g for 10 minutes at 18 °C. Subsequently,

the supernatant was removed and the cell pellet was resuspended in fresh media for another wash and centrifugation cycle. The resulting pellet was finally resuspended in RPMI-1640 medium supplemented with 2 mM L-glutamine, 0.1 mg/ml streptomycin, 100 U/ml penicillin and 10 % autologous serum. The cells were then seeded (for volume see table 2) onto cell culture multiwell plates and incubated at 37 °C under 5 % CO_2 atmosphere. Autologous serum initiates the differentiation of monocytes towards macrophages. The cells were allowed to adhere to the cell culture plate for two hours. During differentiation, the morphology changes from spherical suspension cells to elongated adherent cells. After these two hours, the medium was replaced with a smaller volume of fresh medium (same supplements, for volume see table 2). The next media change was carried out after two days. Until complete differentiation towards macrophages, which was achieved after one week, cells were fed every two days with supplemented medium. After this week, HMDM were ready for use in experiments.

Well format	Growth area per well (cm^2)	Seeding volume per well (ml)	Feeding volume per well (ml)
6 well plate	9.6	4	2
12 well plate	3.9	2	0.75
24 well plate	1.9	1	0.35

Table 2: Seeding and feeding of HMDM in multiwell plates

In general, one EDTA-tube containing 9 ml of full blood was used to seed one well of a 6 well plate or two wells of a 24 well plate.

4.2 Lipoprotein preparation

The lipoproteins used throughout the experiments were isolated from venous blood of healthy, adult fasting volunteers via sequential ultracentrifugation.

4.2.1 Isolation of lipoproteins

Blood was collected in tubes containing EDTA (0.18 M EDTA, pH 8; 2 ml per 50 ml blood) to inhibit the blood coagulation cascade. Then, the EDTA-blood samples were centrifuged at 620 x g for 10 minutes at room temperature without brake. Next, the upper phase, which represents the plasma, was collected and lipoproteins were separated according to Schumaker et al., 1986. In brief, the density of the plasma was

first adjusted to the density of VLDL (i.e. 1.019 g/cm³) with potassium bromide (KBr). For calculation of the required amount of KBr in gram, the following formula was used:

$$g\ KBr = \frac{Volume_{sample}\ (ml) \times (Density_{final} - Density_{initial})}{1 - (0.312 \times Density_{final})}$$

Afterwards, the plasma was filled in centrifuge tubes (Quick-Seal™ centrifuge tubes, Beckman Instruments Inc, Palo Alto, USA) and centrifuged at 51,000 rpm (200,000 x g) in an ultracentrifuge (Optima™ L-100 XP Ultracentrifuge, rotor type: 55.2 Ti, Beckman Coulter, Brea, USA) for 20 hours at 4 °C. Then, VLDL, which was contained in the top fraction, was collected with a syringe after slicing the top of the tube. Afterwards, the remaining plasma fraction (i.e. without VLDL) was adjusted to the density of LDL (1.063 g/cm³) with KBr and centrifuged (same conditions as for VLDL). Following centrifugation, LDL was collected from the top phase of the centrifuge tube and the remaining plasma was adjusted to the density of HDL (1.22 g/cm³). A further centrifugation step was performed in order to collect HDL in the top fraction of the tube. Finally, the collected HDL fraction was centrifuged again for further purification and to ensure complete removal of other constituents such as albumin. LDL and HDL were dialyzed against dialysis buffer (154 mM NaCl, 3 mM EDTA, pH 7.4) for 24 hours at 4 °C to remove KBr from the fractions.

4.2.2 Low-Density-Lipoprotein (LDL) modification

In vitro modification of LDL was performed to obtain carbamylated LDL (cLDL), oxidized LDL (oxLDL) or acetylated LDL (acLDL) as follows:

Carbamylation of LDL was performed via incubation of 2 mg/ml LDL in 50 mM phosphate buffer containing 246.5 mM, 123.25 mM or 61.5 mM KCNO in a reaction volume of at least 100 µl for 4 hours at 37 °C. To remove KCNO from the solution, cLDL was purified via gel exclusion chromatography (illustra™ NICK™ column, GE Healthcare, Buckinghamshire, UK). Therefore, 100 µl cLDL were eluted with 400 µl PBS (phosphate buffered saline, 137 mM NaCl, 2.7 mM KCl, 1.5 mM KH_2PO_4, 8.1 mM Na_2HPO_4, pH 7.4). LDL carbamylated with 246.5 mM KCNO was used for incubation of cells, whereas less carbamylated LDL samples were exclusively used for the analysis of their relative electrophoretic mobility (cpt 4.2.4).

For oxLDL, 2 mg/ml LDL was passed over a NICK™ column to remove EDTA, which is contained in the ultracentrifuged and dialyzed LDL fraction, by chromatography (illustra™ NICK™ column, same procedure as for cLDL) and then incubated with 10 µM $CuSO_4$ for 4 hours at 37 °C. Then, $CuSO_4$ was inactivated by adding 50 µM EDTA in order to chelate copper.

Acetylation of LDL was accomplished by adding LDL (2 mg/ml) to the same volume of saturated sodium-acetate. The mixture was gently stirred on ice and five times, every 10 minutes, acetic acid anhydride (0.01 % (v/v) of the final volume) was added. Then, the solution was gently stirred on ice for additional 30 minutes and afterwards dialyzed against dialysis buffer for 24 hours at 4 °C.

Unmodified LDL (native LDL, nLDL), used as a control, was also run through a NICK™ column for removal of EDTA. All LDL solutions were sterile filtered through a sterile 0.45 µm filter (Arcodisk®, Gelman Sciences, Michigan, USA).

4.2.3 High-Density-Lipoprotein (HDL) modification

HDL was carbamylated *in vitro* using the same method as described for LDL. Therefore, 2 mg/ml HDL were incubated with 50 mM phosphate buffer containing varying concentrations of KCNO for 4 hours at 37 °C. To obtain HDL samples with different degrees of carbamylation, the KCNO concentrations were 246.5 mM, 123.3 mM, 61.6 mM, 30.8 mM 15.4 mM, 7.7 mM and 3.9 mM. After 4 hours of incubation, the cHDL samples were purified from KCNO via gel exclusion chromatography (NICK™ column). 100 µl cHDL were eluted with 400 µl PBS.

Unmodified HDL (native HDL, nHDL) was also run through a NICK™ column for removal of EDTA.

To confirm the results obtained with individual carbamylated HDL samples, another method was used to prepare HDL samples with different amounts of carbamylated particles. Therefore, one HDL sample was carbamylated with 246.5 mM KCNO as described above. The cHDL sample was further diluted stepwise 1:1 with nHDL to yield nine less carbamylated samples.

4.2.4 Analysis of the relative electrophoretic mobility of carbamylated lipoproteins by agarose gel electrophoresis

Carbamylation changes the electrophoretic properties of proteins. The modification of lysine amino groups of proteins leads to the removal of positive charge from the protein and therefore, the electrophoretic mobility of carbamylated proteins differs from their native forms (for review see Jaisson et al., 2011).

Native and carbamylated samples of LDL and HDL were loaded onto a 1 % agarose gel. For agarose gel preparation, 1 % agarose was dissolved in TAE buffer (Tris-Acetate-EDTA; 40 mM Tris, 20 mM acetic acid, 1 mM EDTA, pH 8.0) and boiled in a microwave. The gel was poured into a gel-tray and a 8-well comb was inserted. After assembly, the electrophoresis chamber was filled with TAE buffer. The comb was removed from the gel and samples (each containing 10 µg protein) with loading dye (6x DNA loading dye; Fermentas GmbH, St. Leon-Rot, Germany) were loaded into the slots. Electrophoresis was performed at 90 Volts for 90 minutes. Subsequently, the gel was stained with Coomassie staining solution composed of 0.1 % Coomassie blue, 30 % methanol and 10 % acetic acid for 15 minutes. Afterwards, the gel was destained in 20 % methanol, 10 % acetic acid, 70 % ddH_2O overnight. Finally, the gel was photographed for further analysis of the relative electrophoretic mobility (REM).

4.2.5 Assessment of carbamylation

The degree of carbamylation in lipoprotein preparations was measured using a colorimetric method (Trepanier et al., 1996). Therefore, 20 µg of lipoprotein were digested in a volume of 50 µl containing PBS (pH 7.4), 2 µg proteinase K and 1 % sodium dodecyl sulfate (SDS) at 37 °C for 2 hours. Afterwards, 250 µl of urea-nitrogen-reagent (0.83 M sulfuric acid, 1.13 M orthophosphoric acid, 0.55 mM thiosemicarbazide, and 2.6mM cadmium sulfate) and 50 µl diacetyl monoxime (3 % in ddH_2O) were added and incubation continued at 97 °C for 30 minutes. To remove precipitates, the samples were centrifuged at 3500 x g for 10 minutes at room temperature. The supernatant was transferred to a new tube and centrifuged again for complete removal of precipitates. Then, 200 µl of the supernatant was transferred into a 96-well plate and absorption was measured at 535 nm. A standard curve was created using 0, 1.875, 3.73, 7.5, 15 and 30 nmol ε-amino-carbamyllysine (L-homocitrulline (Hcit), Chemos GmbH, Regenstauf, Germany) in the particular

standard. Standards underwent the same treatment as samples. The measurements of the samples were interpolated from the standard curve and expressed in µmol Hcit/g protein.

4.3 Protein determination

For determination of protein the Bio-Rad Protein Assay (Bio-Rad Laboratories GmbH, Munich, Germany) was used. The assay is based on the observation that binding of an acidic solution of Coomassie Brilliant Blue G-250 to protein shifts the absorbance maximum from 465 nm to 595 nm (Bradford, 1976).

For this purpose, 1-10 µl of a sample with unknown protein concentration was added to 20 µl Bio-Rad Protein Assay reagent placed in a 96-well plate and filled up with distilled water to a total volume of 100 µl. To create a standard curve consisting of known protein concentrations, bovine serum albumin (BSA) was used. Absorbance at 595 nm was measured in a microplate reader (Bio-Rad, iMark™ microplate reader) after 5 to 30 minutes. The concentrations of the unknown protein samples were interpolated from the standard curve.

4.4 RNA isolation from THP-1 cells

RNA was isolated from THP-1 cells using the RNeasy® Plus Micro Kit (Qiagen, Hilden, Germany). Therefore, the cells were washed twice with PBS and then exposed to 350 µl RLT Plus buffer including 1% β-mercaptoethanol for disruption. Then, the lysate was passed several times through a 20-gauge needle (0.9 mm diameter) fitted to a syringe for homogenization. To obtain an efficient cell lysis, the lysates were frozen at -80 °C until further processing. After thawing, the isolation procedure was performed as described by the manufacturer. Finally, RNA was eluted with 15 µl RNase free water and the concentration of each sample was determined spectrophotometrically (NanoDrop® ND-1000, NanoDrop Technologies, Wilmington, USA). RNA was stored at -80 °C until further use. From cells seeded in a well of a 12 well plate (3.9 cm^2 growth area per well), 120 to 3600 ng RNA were recovered (dependent on cell confluency).

4.5 MicroRNA isolation from THP-1 cells

The isolation of miRNA from THP-1 cells was performed using the miRNeasy® Mini Kit (Qiagen, Hilden, Germany). For this purpose, cells were washed twice with PBS before lysis with QIAzol Lysis Reagent. The lysate was homogenized by passing it several

times through a 20-gauge needle (0.9 mm diameter) fitted to a syringe. Further processing for miRNA isolation was performed as described by the manufacturer. Finally, miRNA was eluted with 75 µl RNase free water, the concentration was determined spectrophotometrically and stored at -80 °C until further use. From the cells seeded in one well of a 6 well plate (9.6 cm^2 growth area per well), 120 to 3600 ng miRNA were recovered (dependent on cell confluency).

4.6 Reverse Transcription PCR

All reagents and materials used in reverse transcription PCR and quantitative real-time PCR were obtained from Applied Biosystems (Foster City, USA) unless noted otherwise.

4.6.1 Reverse transcription of RNA to cDNA

To convert RNA into cDNA, RNA was reverse transcribed using the High Capacity cDNA Reverse Transcription Kit according to the supplier's protocol. Briefly, a 2X master mix including 10X Reverse Transcription (RT) Buffer, 25X dNTP Mix (100 mM), 10X RT Random Primers, MultiScribe™ Reverse Transcriptase (50 U/µl), RNase Inhibitor (20 U/µl) and nuclease-free water was prepared on ice with a total volume of 10 µl per reaction as follows (table 3):

Reagent	µl
10X RT Buffer	2.0
25X dNTP Mix	0.8
10X RT Random Primers	2.0
Reverse Transcriptase	1.0
RNase Inhibitor	1.0
Nuclease-free Water	3.2
Total volume	10.0

Table 3: RNA reverse transcription master mix

To prepare the cDNA reverse transcription reaction, 140 ng RNA in 10 µl was added to 10 µl 2X master mix. The samples were placed into a thermocycler programmed for the conditions as instructed in the supplier's protocol (see table 4). cDNA was stored at -20 °C until analyzed by quantitative real-time PCR.

	Step 1	Step 2	Step 3	Step 4
Temperature (° C)	25	37	85	4
Time	10 min	120 min	5 min	∞

Table 4: Thermal cycler conditions for reverse transcription of RNA

4.6.2 Reverse transcription of miRNA to cDNA

TaqMan® MicroRNA Reverse Transcription Kit was used for reverse transcription of miRNA to cDNA as outlined in the supplier's manual. In brief, a master mix composed of 100 mM dNTPs, Multiscribe™ Reverse Transcriptase (50 U/µl), 10X Reverse Transcription Buffer, RNase Inhibitor (20 U/µl) and nuclease-free water was prepared on ice as described in table 5.

Reagent	µl
100 mM dNTPs	0.15
Reverse Transcriptase	1.00
10X RT Buffer	1.50
RNase Inhibitor	0.19
Nuclease-free Water	1.16
Master mix - total volume	4.00

Table 5: miRNA reverse transcription master mix

3 µl of the corresponding 5X TaqMan® MicroRNA Assay (see table 6) was added to the master mix. Additionally, 3 µl of 5X RT Primer miR-16 or RNU44 was added to each reverse transcription assay as endogenous controls during real-time PCR.

5X TaqMan® MicroRNA Assay (Applied Biosystems)	ID
hsa-miR-16	RT:000391
RNU44	RT:001094
hsa-miR-223	RT:002295
hsa-miR-33a	RT:002135

Table 6: Primers used for miRNA conversion
(the prefix "hsa" stands for "homo sapiens" for species designation)

To this 10 µl reaction mix, 100 ng miRNA in 5 µl was added for preparation of the cDNA reverse transcription. The samples were incubated on ice for 5 minutes and afterwards placed into a thermal cycler programmed for the conditions as described in the supplier's protocol (see table 7). Until performing quantitative real-time PCR, the cDNA samples were stored at -20 °C.

	Step 1	Step 2	Step 3	Step 4
Temperature (° C)	16	42	85	4
Time	30 min	30 min	5 min	∞

Table 7: Thermal cycler conditions for reverse transcription of miRNA

4.7 Measurement of mRNA expression by quantitative real-time PCR

Quantitative real-time PCR (qPCR) experiments were performed to investigate the effect of different concentrations of cLDL and nLDL on ABCA1, ABCG1, SR-BI (SCARB1) and LXRα (NR1H3) mRNA expression. Additionally, ABCA1, ABCG1, SR-BI and LXRα mRNA levels were quantified during different time points of THP-1 differentiation via qPCR.

For quantitative real-time PCR, 2 µl reverse transcribed RNA (14 ng) were added to 7.5 µl TaqMan® Gene Expression Master Mix, 0.756 µl of the corresponding TaqMan® Gene Expression Assay (table 8) and 4.75 µl nuclease-free water resulting in a final volume per reaction of 15 µl.

TaqMan® Gene Expression Assay (Applied Biosystems)	ID
ABCA1	Hs00194045_m1
ABCG1	Hs01555193_m1
SCARB1	Hs00969821_m1
NR1H3	Hs00172885_m1
18S	Hs99999901_s1

Table 8: Description of primers used for qPCR (mRNA)

Samples were measured in duplicates in a 48-well reaction plate (MicroAmp™ Fast Optical 48-Well Reaction Plate) sealed with adhesive film (MicroAmp™ 48-Well Optical Adhesive Film). Negative control samples contained nuclease-free water instead of cDNA. TaqMan® Gene Expression Assays for reverse transcribed 18S rRNA were used as endogenous control and cDNA from cells treated with BSA were used as reference sample. After sealing with adhesive film, the plate was centrifuged for 1 minute at 1800 x g to eliminate any air bubbles and for spinning down the contents. Then, the plate was placed in a real-time PCR system (StepOne™ Real-Time PCR System) to start the PCR reactions according to the thermal cycling program (see table 9) of the supplier's protocol. Before starting the real-time PCR system, the setup of the plate was defined via the StepOne™ Software (Version 2.1). The experiment type was set to "Quantitation – Comparative C_T ($\Delta\Delta C_T$)", as the expression of 18S rRNA was used as endogenous control for relative quantitation (RQ) of the respective target (ABCA1, ABCG1, SR-BI or LXRα mRNA) contained in the sample relative to the

reference sample (BSA incubation). After completion of the run, the C_T values were used for relative quantitation.

	UDG incubation	Polymerase activation	PCR	
	Hold	Hold	Cycle (40 cycles)	
			Denature	Anneal/extend
Temperature (° C)	50	95	95	60
Time	2 min	10 min	15 sec	1 min

Table 9: Thermal cycler conditions for quantitative real-time PCR (mRNA)

UDG (uracil-DNA glycosylase), contained in the TaqMan® Gene Expression Master Mix, prevents reamplification of carryover-PCR products (from the reverse transcription reaction) during the assay as outlined in the manufacturer's manual.

4.8 Measurement of miRNA expression by quantitative real-time PCR

For analyzing the effect of cLDL, oxLDL, acLDL and nLDL on miRNA gene expression of miR-223 and miR-33a in THP-1 cells, quantitative real-time PCR was performed. For this purpose, 1.33 µl of reverse transcribed miRNA (i.e. 8.9 ng) were incubated with 10 µl TaqMan® Universal Master Mix II (without UDG), 7.67 µl nuclease-free water and 1 µl of the corresponding 20X TaqMan® MicroRNA Assay (table 10) to give a total volume of 20 µl per reaction.

20X TaqMan® MicroRNA Assay (Applied Biosystems)	ID
hsa-miR-16	TM:000391
RNU44	TM:001094
hsa-miR-223	TM:002295
hsa-miR-33a	TM:002135

Table 10: Primers used for qPCR (miRNA)

The rest of the procedure was similar to qPCR of mRNA (see above). Samples were applied in duplicates on a 48-well reaction plate (MicroAmp™ Fast Optical 48-Well Reaction Plate) and sealed with adhesive film (MicroAmp™ 48-Well Optical Adhesive Film) to avoid evaporation and contamination. Negative control samples contained nuclease-free water only instead of cDNA. TaqMan® MicroRNA Assays for miR-16 and RNU44 were used as endogenous controls and the cDNA of cells incubated with BSA was used as reference sample. To spin down the contents and for elimination of any air bubbles, the plate was centrifuged for 1 minute at 1800 x g.

Before starting the reactions with simultaneous measurement in a real-time PCR system (StepOne™ Real-Time PCR System), the plate setup was defined in the StepOne™ Software (Version 2.1). The type of experiment was set to "Quantitation – Comparative C_T ($\Delta\Delta C_T$)", as an endogenous control (miR-16 or RNU44) was used for relative quantitation of the respective target (miR-223 or miR-33a) in the sample relative to the reference sample (BSA incubation). The thermal cycling conditions of the real-time PCR system were set according to the instructions of the manufacturer's protocol (see table 11). After completion of the run, the C_T values were used for relative quantitation.

	Polymerase activation	PCR	
	Hold	Cycle (40 cycles)	
		Denature	Anneal/extend
Temperature (° C)	95	95	60
Time	10 min	15 sec	1 min

Table 11: Thermal cycler conditions for quantitative real-time PCR (miRNA)

4.9 Western Blotting

4.9.1 Cell lysis

THP-1 macrophages or HMDM on 6-well plates were placed on ice and washed twice with cold (4 °C) PBS. For lysis, cells were incubated with 40-80 µl (depending on cell confluency) membrane lysis buffer (62.5 mM Tris pH 6.8, 8 M urea, 20 mM EDTA, 20 mM EGTA, 10 % glycerol, 1 % SDS) supplemented with protease inhibitor cocktail (1:100; Sigma, catalog number: P8340) for 10 minutes. Afterwards, the cells were scraped with a rubber policemen for efficient detachment from the bottom of the well. Then, the lysates were transferred to an Eppendorf tube, sonicated for 5 seconds, incubated on ice for one hour and stored at -20 °C for at least one week to increase lysis efficiency. Then, samples were thawed on ice for one hour and then centrifuged at 14,000 x g for 10 minutes to remove any precipitates. The supernatant was transferred into a new tube and the protein concentration was determined using the Bradford Assay (see cpt. 4.3).

4.9.2 Sample preparation

Samples were prepared for SDS-PAGE by diluting equal amounts of protein (7 µg protein per lane on SDS gel) with PBS. Proteins were denaturated by adding freshly

prepared 4X sample buffer (50 % glycerol, 45 % 0.5 M Tris-HCl pH 6.8 with 8 % SDS, 5 % β-mercaptoethanol, dash of bromphenol blue) with subsequent incubation for 30 minutes at 40 °C. The samples were allowed to reach room temperature before they were loaded onto the gel.

4.9.3 SDS-PAGE

The Mini-PROTEAN 3 Cell (Bio-Rad) was used for gel preparation according to the manufacturer's handbook.

For the resolving gel (8%) the first three components listed in table 12 were mixed. As APS and TEMED start the polymerization reaction of the gel, both substances were added immediately before pouring the gel. Proper mixing of all ingredients was assured by vortexing. After casting the resolving gel between a short glass plate and a 0.75 mm spacer plate, it was overlaid instantly with isopropanol to prevent the gel from drying out and to avoid air contact and thereby ensuring complete polymerization. After 30 minutes, the resolving gel was polymerized, isopropanol was removed and the prepared stacking gel solution (4 %, composition described in table 12) was poured onto the resolving gel. Finally, a 15-well comb was inserted between the glass plates and the gel was allowed to polymerize for another 30 minutes.

	Resolving gel (8 %)	Stacking gel (4 %)
ddH_20	1.6 ml	1.1 ml
30 % acrylamide/N,N'-methylene-bis-acrylamide (29.2:0.8)	1.1 ml	0.3 ml
3 M Tris-HCl pH 8.45, 0.3 % SDS	1.3 ml	0.7 ml
10 % APS	30 µl	20 µl
TEMED	3 µl	2 µl

Table 12: Components of SDS-PAGE gel (for 1 gel 72x100 mm, spacer 0.75 mm)

After complete polymerization, the gel cassettes were inserted into the electrophoresis module. Tris/Glycine buffer (25 mM Tris, 192 mM glycine, 0.1 % SDS, pH 8.3) was used as electrophoresis buffer. The comb was removed from the gel and the slots were rinsed with electrophoresis buffer. The slots were loaded with the samples (cpt. 4.9.2) and a protein ladder (Spectra™ Multicolor High Range Protein Ladder, Fermentas GmbH) and empty slots were filled with sample buffer.

Electrophoresis was carried out at 4 °C for 85 minutes at a constant voltage of 180 Volts. After completion of the run, the gel cassette was removed from the electrophresis module and the gel was detached from the glass plates for transfer.

4.9.4 Electrophoretic transfer

The gel was blotted onto a nitrocellulose membrane (0.45 µm, Bio-Rad) using the Mini Trans-Blot® Electrophoretic Transfer Cell (Bio-Rad) according to the manufacturer's manual. The transfer sandwich unit was assembled as described in the instructions as follows:

White side of gel holder cassette Fiber pad Filter paper Nitrocellulose membrane Gel Filter paper Fiber pad Black side of gel holder cassette

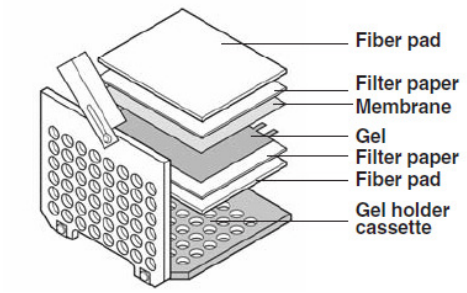

Table 13: Assembly of transfer sandwich for Western blot according to the supplier's instructions

Prior to assembly, fiber pads, filter paper and the nitrocellulose membrane were wetted with Transfer Buffer (Tris/Glycin Buffer, 20 % methanol). Any air bubbles between nitrocellulose membrane and gel were rolled out with a glass tube.

After complete assembly of the transfer sandwich, the gel holder cassette was locked and placed in the electrophoresis module together with an ice block to ensure cooling during transfer. Then the transfer was performed at 4 °C for 43 minutes with a constant electric current of 0.4 ampere.

Subsequent to the transfer, the nitrocellulose was incubated with Ponceau S staining solution (1 % Ponceau S, 30 % trichloroacetic acid, 30 % sulfosalicylic acid) for 5 minutes to visualize proteins. Thereafter, excess staining solution was removed, the nitrocellulose was rinsed with deionized water and was cut according to the molecular mass of proteins studied, as indicated by the protein ladder. Afterwards, the nitrocellulose membrane strips were washed with Tris-Buffered Saline Tween (TBS-T; 20 mM Tris, 145 mM NaCl, 0.1 % Tween-20, pH 7.4) for 10 minutes to completely remove Ponceau S staining solution.

4.9.5 Immunological detection of proteins

To block nonspecific sites, the nitrocellulose membrane strips were incubated with blocking buffer (TBS-T with 5 % nonfat dry milk, Maresi, Vienna, Austria) for 1 hour. After blocking, the strips were washed three times (10 minutes each) with TBS-T and incubated with the respective primary antibody solution (table 14) overnight at 4 °C.

Antibody (species reactivity: human)	Host	Supplier	Product ID	Position of protein band	Dilution
Anti-ABCA1 (polyclonal)	rabbit	Novus Biologicals LCC, Littleton, USA	NB400-105	~ 220 kDa	1:500 in TBS-T with 3 % BSA
Anti-ABCG1 (polyclonal)	rabbit	Novus Biologicals LCC	NB400-132	~ 76 kDa	1:2000 in TBS-T with 3 % BSA
Anti-SR-BI (polyclonal)	rabbit	Novus Biologicals LCC	NB400-104	~ 82 kDa	1:3000 in TBS-T with 2.5 % nonfat dry milk
Anti-β actin (monoclonal)	mouse	Sigma Aldrich	A2228	~ 42 kDa	1:3000 in TBS-T with 3 % BSA

Table 14 : Primary antibodies used for Western blot

A dash of sodium azide was added as preservative to all primary antibody solutions. The solutions were stored at 4 °C and were reused several times.

After overnight incubation of the nitrocellulose membranes, the primary antibody solutions were removed and the membranes were washed three times (10 minutes each) with TBS-T. Next, incubation with secondary antibody was carried out. Therefore, all secondary antibody solutions were freshly prepared in blocking buffer. For the ABC-transporters (ABCA1 and ABCG1) and SR-BI, Goat Anti-Rabbit IgG-HRP Conjugate (Bio-Rad) was diluted 1:8000 or 1:11250, respectively, in blocking buffer. For β-actin, Goat Anti-Mouse IgG-HRP Conjugate (Bio-Rad) was diluted 1:15000 in blocking buffer. The respective nitrocellulose membrane strips were incubated with secondary antibody solutions for 1 hour at room temperature. Another three washes with TBS-T followed after exposure to secondary antibody.

Thereafter, a chemiluminescence working solution (SuperSignal West Dura Extended Duration Substrate, Thermo Fisher Scientific Inc., Rockford, USA) was prepared by

mixing equal parts of the Stable Peroxide Solution and the Luminol/Enhancer Solution. The nitrocellulose membranes were incubated with working solution for 5 minutes and afterwards, excess liquid was removed. Finally, the membrane was placed below a CCD camera in a dark chamber of an image acquisition system (Fusion FX7; Peqlab Biotechnologie GmbH, Erlangen, Germany). For detection, an adequate light exposure-time of the instrument was chosen. The resulting images were quantified using the software AlphaEaseFC™ (Alpha Innotech Corporation, USA).

As β-actin was used as loading control, each band of ABCA1, ABCG1 and SR-BI was normalized to the respective β-actin band.

4.10 Cholesterol efflux measurements

Cholesterol efflux experiments were conducted under different circumstances. First, it was investigated whether cLDL-treated macrophages have an altered cholesterol efflux compared to nLDL-treated macrophages and second, the cholesterol acceptor capacities of carbamylated HDL versus native HDL as well as the cholesterol acceptor capacities of serum from CRF and ESDR patients versus serum from healthy controls were studied.

4.10.1 Measurement of the effect of carbamylated LDL on the cholesterol efflux capacity of macrophages

THP-1 macrophages and differentiated HMDM, grown on 24-well plates, were incubated with either cLDL or nLDL (both 50 µg/ml) for 48 hours. 24 hours prior to the efflux experiment, 0.5 µCi [^{3}H]-cholesterol (PerkinElmer Inc, Waltham, USA) was added per well. Then, cholesterol efflux was measured to apoA-I (Meridian Life Science® Inc, Memphis, USA), HDL (obtained according to the method of cpt 4.2.1), serum (obtained from blood of an healthy adult volunteer) and medium. Therefore, the cells were washed twice with PBS, and subsequently, the macrophages were equilibrated for 2 hours with 250 µl medium per well. Then, the cells were incubated with 250 µl/well RPMI-1640 without supplementation or RPMI-1640 supplemented with either apoA-I (10 µg/ml), HDL (10 µg/ml), or serum (1 %) for 6 hours at 37 °C. Thereafter, the supernatant from the cells was collected and centrifuged at 4 °C for 10 minutes at 500 x g to remove any cell components. The cells were washed twice with PBS and lysed with 250 µl/well 0.1 M NaOH for 1 hour at room temperature. Both, the [^{3}H]-cholesterol contained in the cell lysate and the release of [^{3}H]-cholesterol into the

cell supernatant were analyzed by scintillation counting. For this purpose, 150 µl of the respective cell lysate or centrifuged supernatant was added to 15 ml scintillation fluid (BioFluor Plus™, PerkinElmer). The samples were measured in a β-counter (Tricarb 2800 TR Liquid Scintillation Analyzer, PerkinElmer) for determination of disintegrations per minute (dpm). From the remaining cell lysate, protein determination using Bradford assay (cpt. 4.3) was carried out.

Cholesterol efflux from the cells to the particular acceptor (apoA-I, HDL, serum) was expressed in percent of the total dpm (total = dpm of supernatant + dpm of lysate). Further, the efflux to medium only (i.e. nonspecific efflux) was subtracted from the efflux to the respective acceptors to obtain specific efflux.

Furthermore, the same experiment was performed with THP-1 cells after blocking the ABCA1-mediated cholesterol efflux by probucol as described by Favari et al., 2004. Cells were treated with a 10 µM probucol solution during the 2 hour equilibration phase. For the probucol working solution, a stock solution (10 mM probucol) was prepared in ethanol, which was stored at -20 °C and reused for further experiments. Further dilution of the stock solution was carried out in RPMI-1640 supplemented with 4 % BSA (to maintain solubility) to obtain a concentration of 200 µM probucol. Finally, the solution was further diluted to the working solution with RPMI-1640, yielding a final concentration of 10 µM probucol, 0.1 % ethanol and 0.2 % BSA. For control incubations, cells were treated with the same solution without probucol.

4.10.2 Measurement of the cholesterol acceptor capacity of HDL and serum

Differentiated THP-1 macrophages, cultured on 24-well plates, were incubated with 50 µg/ml acLDL for cholesterol-loading and 3 µM of T0901317 (synthetic LXR-Agonist for upregulation of ABCA1 and ABCG1) and were trace-labeled with 0.5 µCi [^{3}H]-cholesterol 24 hours prior to the efflux experiment. On the day of the efflux experiment, cells were washed with PBS, equilibrated with medium and afterwards incubated with 10 µg/ml carbamylated HDL for 6 hours. The cHDL samples were carbamylated to obtain different degrees of carbamylation (see cpt. 4.2.3). Efflux was measured as described above (cpt. 4.10.1).

A similar experiment was performed with differentiated HMDM. These cells were also incubated with acLDL, [^{3}H]-cholesterol and T0901317 (same concentrations as for THP-1) the day before the efflux experiment. After washing with PBS and equilibration

with medium, the cells were incubated with 10 µg/ml cHDL (carbamylated with 246.5 mM KCNO), 10 µg/ml nHDL or medium for 6 hours to measure efflux.

Another field of interest was to determine the efflux capacity of serum of patients (cpt. 4.11) with CRF or ESRD on hemodialysis treatment compared to the efflux capacity of serum of healthy controls. Therefore, THP-1 macrophages and HMDM were treated with 50 µg/ml acLDL, 0.5 µCi [^{3}H]-cholesterol and 3 µM T0901317 for 24 hours. Cells were washed with PBS and equilibrated with medium for 2 hours prior to incubation with medium supplemented with 1 % serum of patients or respective healthy controls for 6 hours. Afterwards, efflux was measured as described above. Efflux of HMDM was measured to pooled serum of the respective groups in 4 independent experiments.

4.11 Patients

For this study 17 adult patients suffering from CRF KDOQI (National Kidney Foundation Kidney Disease Outcomes Quality Initiative) stage 3-5 without hemodialysis and 14 adult CRF patients on maintenance hemodialysis and matched controls were recruited (see table 15 for details). The study was approved by the Ethics Committee of the Medical University of Vienna (Protocol # 511/2007). Written informed consent was obtained from all participants. Patients with diabetes mellitus, nephrotic syndrome, inflammatory diseases, malignancy and infections within the last 3 months, and patients on corticosteroids, lipid lowering or immunosuppressive drugs were excluded. 20-30 ml of venous blood was collected after an overnight fast. EDTA plasma was stored at 4 °C for lipoprotein isolation and serum was frozen in aliquots at -20 °C for lipid and apolipoprotein analysis. Monocytes were isolated from EDTA blood and differentiated towards macrophages.

4.12 Statistical Analysis

Data analysis was performed using the statistical software package GraphPad Prism® Version 5.00 (GraphPad Software Inc., La Jolla, USA). Data are expressed as means ± standard deviation (SD) and analyzed via unpaired t-test, one-way analysis of variance (ANOVA) with Newman-Keuls post test or two-way ANOVA with Bonferroni post test. Differences were considered statistically significant if $p < 0.05$.

5 Results

5.1 Characterization of carbamylated lipoproteins

In vitro carbamylated lipoproteins were analyzed regarding their change in electrophyoretic mobility as well as their degree of carbamylation via a colorimetric assay as quality control experiments.

5.1.1 Relative electrophoretic mobility of carbamylated and native lipoproteins

As carbamylation increases the overall negative charge of a protein, carbamylated proteins have different eletrophoretic mobilities compared to uncarbamylated proteins. Thus, carbamylated proteins move faster towards the positive pole during agarose gel electrophoresis (Kraus et al., 2001).

To investigate the change in electrophoretic mobility, agarose gel electrophoresis of liporoteins, carbamylated with different concentrations of potassium cyanate, was performed. In this assay, the electrophoretic mobilities of the native forms of LDL and HDL (lane 1 and lane 5, respectively, see figure 3) were set to 1.

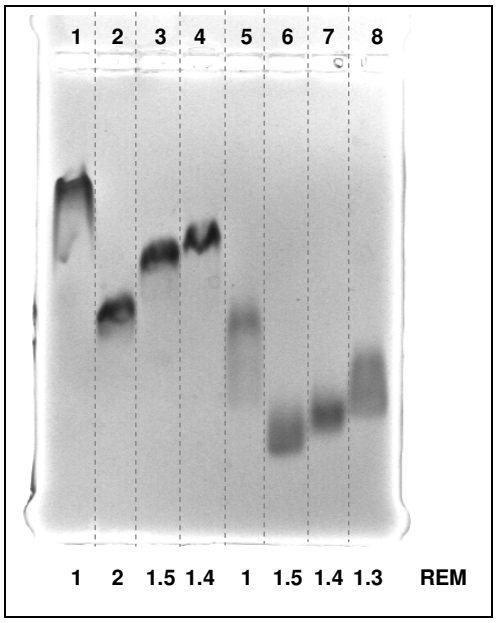

Figure 3: Relative electrophoretic mobility of carbamylated lipoproteins
Cathode is at the top of the figure.
Lipoproteins were applied as follows:
nLDL (lane 1),
LDL carbamylated with 246.5 mM (lane 2), 123.25 mM (lane 3), 61.6 mM (lane 4) KCNO
nHDL (lane 5),
HDL carbamylated with 246.5 mM (lane 6), 123.25 mM (lane 7), 61.6 mM (lane 8) KCNO

For both, LDL and HDL, REM increased with increasing KCNO concentration used for carbamylation. Concerning LDL, the REM (indicated in figure 3) of the highest carbamylated sample doubled in comparison to its native form and decreased when carbamylation decreased. A similar pattern could be recognized for HDL, the highest KCNO concentration resulted in an REM of 1.5.

5.1.2 Assessment of carbamylation

The degree of carbamylation of HDL and LDL samples was determined by a colorimetric method using diacetyl monoxime as described in cpt 4.2.5. HDL and LDL samples were carbamylated with the respective KCNO concentrations (indicated in figure 4 and figure 5) for analysis.

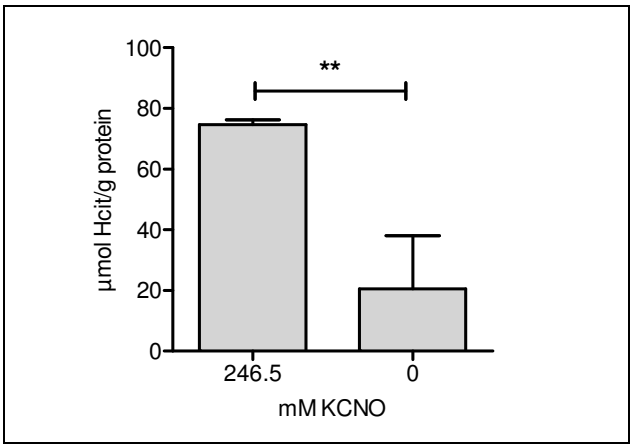

Figure 4: Assessment of carbamylation of carbamylated (left) and native (right) LDL (n=3, mean ± SD, ** $p < 0.01$, unpaired t-test).

LDL carbamylated with 246.5 mM KCNO had ~3.6 fold more protein bound Hcit compared to its native form (0 mM KCNO, figure 4).

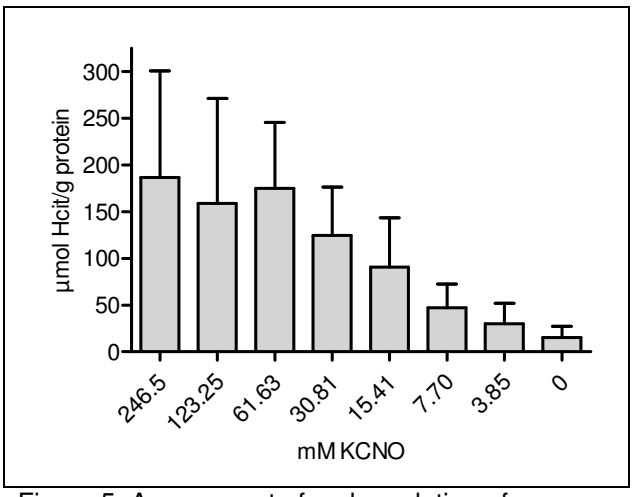

Figure 5: Assessment of carbamylation of carbamylated and native HDL (n=3, mean ± SD).

Furthermore, HDL carbamylated with different concentrations of KCNO was analyzed (figure 5). Here, protein bound Hcit increased with increasing KCNO concentrations used for carbamylation. Native HDL and native LDL showed similar degrees of

carbamylation (both ~20 µmol Hcit/g protein). However, the highest KCNO concentration used during carbamylation resulted in an higher degree of carbamylation (~2.5 fold) of HDL compared to LDL. Both, the results obtained from gel electrophoresis and colorimetric assay confirm that the *in vitro* carbamylation procedure was effective.

5.2 Effect of carbamylated LDL on macrophage cholesterol efflux

To investigate whether incubation with cLDL induces a change in cholesterol efflux as compared to nLDL as response to excessive cholesterol uptake, THP-1 macrophages and HMDM were incubated with 50 µg/ml cLDL or nLDL for 48 hours. Cells were trace-labeled with [^{3}H]-cholesterol for measurement of cholesterol efflux to the cholesterol acceptors apoA-I, HDL and serum.

5.2.1 Cholesterol efflux from THP-1 macrophages incubated with cLDL

Cholesterol efflux to apoA-I was significantly increased in THP-1 macrphages treated with cLDL compared to nLDL treated THP-1 cells as depicted in figure 6. In contrast, efflux to HDL or serum did not differ between treatments. However, a trend to a decreased efflux of cLDL treated THP-1 cells might be recognized to both cholesterol acceptors, HDL and serum. It has to be noticed, that among the cholesterol acceptors studied, most cholesterol (~35 % of total radioactivity) was transported to serum which comprises many cholesterol acceptors. Among them is apoA-I which accounts for ~2-5 % (of total radioactivity) cholesterol uptake.

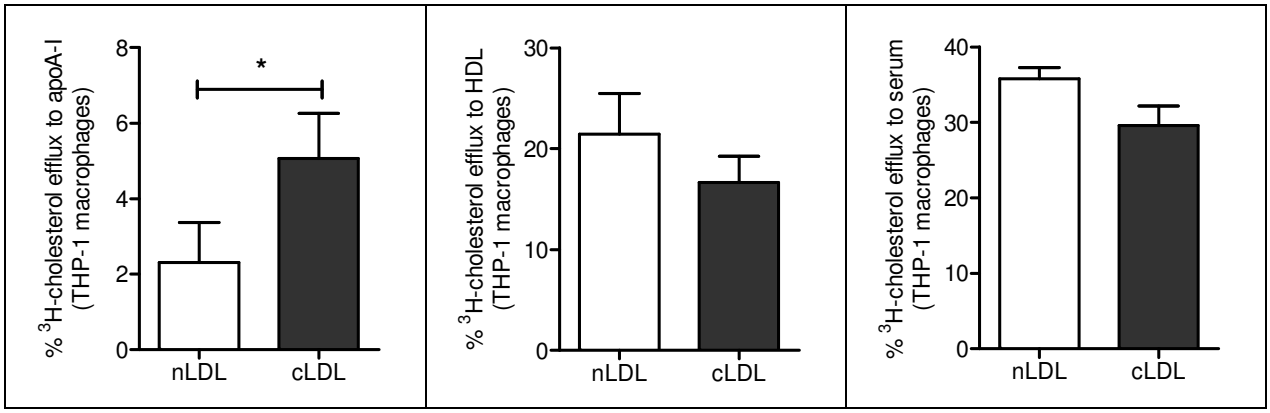

Figure 6: Cholesterol efflux from THP-1 macrophages incubated with nLDL and cLDL
Left panel: efflux to 10 µg/ml apoA-I, middle panel: efflux to 10 µg/ml HDL, right panel: efflux to 1 % serum (n=3, mean ± SD, * $p < 0.05$, unpaired t-test).

5.2.2 Cholesterol efflux from HMDM incubated with cLDL

To confirm the data obtained with THP-1 macrophages, cholesterol efflux experiments using HMDM were performed under the same conditions. Treatment of HMDM with cLDL as compared to nLDL neither influenced cholesterol efflux to HDL nor to serum (figure 7). HMDM, which were treated with cLDL, tended to show an increased efflux to apoA-I in comparison to nLDL treated cells, even though this effect was not significant.

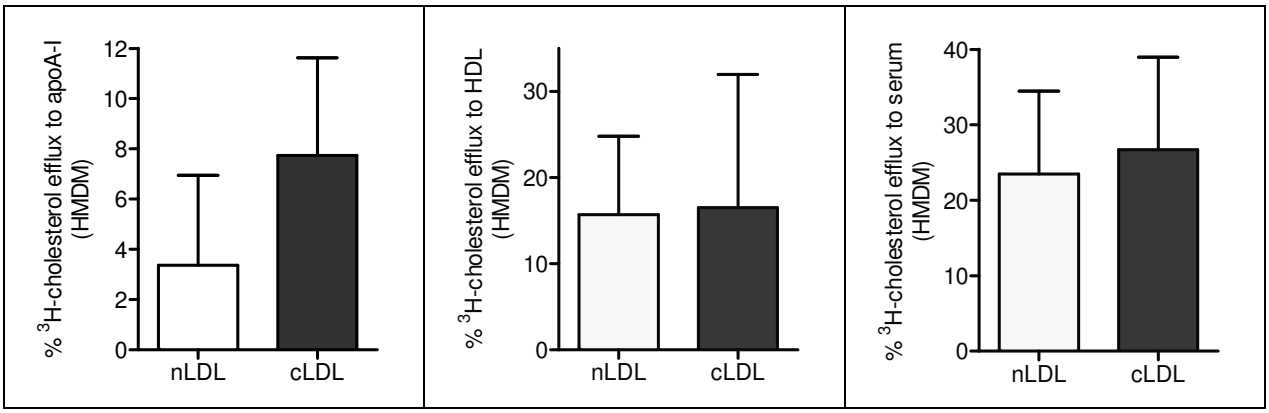

Figure 7: Cholesterol efflux from human monocyte-derived macrophages incubated with nLDL and cLDL Left panel: efflux to 10 µg/ml apoA-I, middle panel: efflux to 10 µg/ml HDL, right panel: efflux to 1 % serum (n=3, mean ± SD).

5.3 Effect of carbamylated and native LDL on ABCA1, ABCG1, SR-BI and LXRα expression in THP-1 macrophages

Incubations of THP-1 macrophages with cLDL increased the cholesterol efflux to apoA-I (cpt 5.2.1) but not to HDL or serum. For validation of any dose-dependent effects of cLDL and/or nLDL on ABCA1, ABCG1, SR-BI and LXRα mRNA and protein expression, THP-1 macrophages were incubated with 12.5, 25, 50 or 100 µg/ml of cLDL or nLDL for 48 hours. BSA (2 mg/ml) incubation was used as control. For evaluation, values obtained from control incubations (BSA) were set to 100 % for Western blot and RQ 1 for qPCR results.

5.3.1 Effect of carbamylated and native LDL on ABCA1 expression

A significant difference between nLDL and cLDL treatment on ABCA1 expression could be recognized only on the mRNA level (figure 8, left panel) measured by quantitative real-time PCR. Four independent incubation experiments showed that cLDL incubation markedly increased ABCA1 mRNA compared to nLDL incubation. ABCA1 mRNA was increased ~1.4 fold when cells were treated with 12.5 µg/ml cLDL and ~1.8 fold when incubated with 100 µg/ml, whereas nLDL treatment did not change

mRNA expression compared to control. This effect seemed to be dose-dependent within the investigated range (from 12.5 to 100 µg/ml LDL) as increasing concentrations of cLDL led to moderately increasing ABCA1 mRNA concentrations.

Considering ABCA1 protein expression measured by Western blot, the obtained results were ambiguous and not statistically significant. However, a trend towards an increase in ABCA1 protein expression was apparent as indicated in figure 8 (right panel). This trend could be seen already when THP-1 macrophages were incubated with a concentration of 25 µg/ml cLDL.

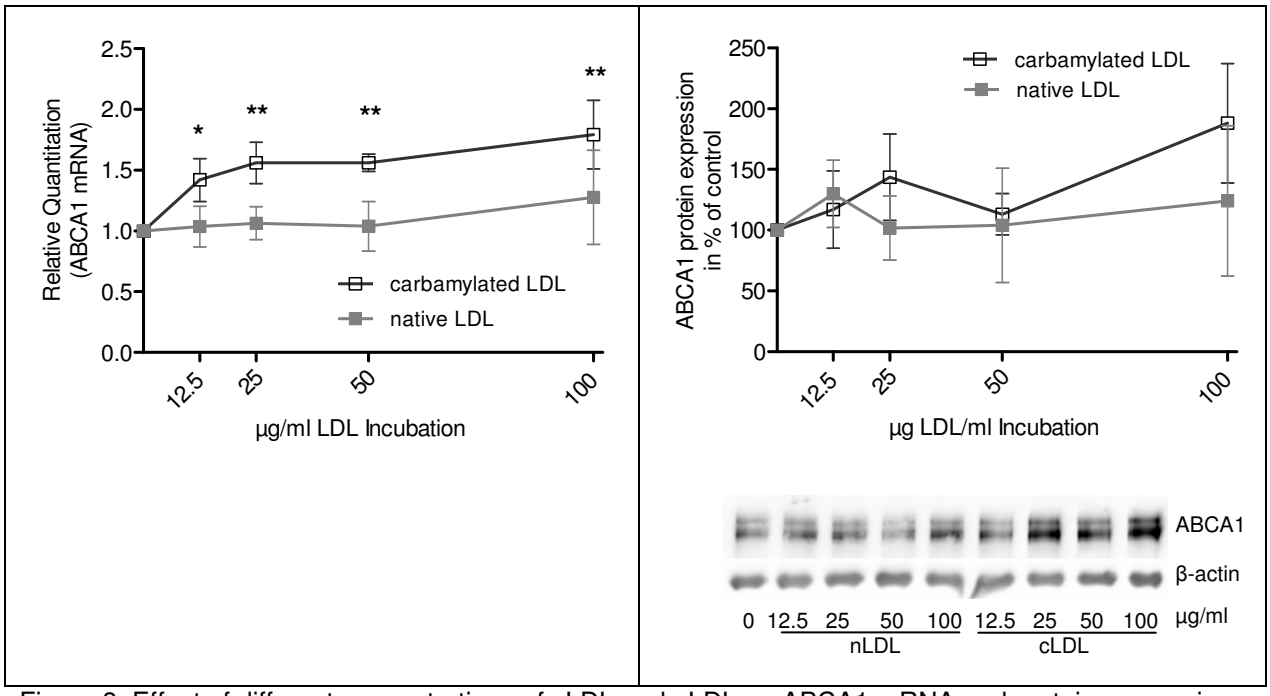

Figure 8: Effect of different concentrations of cLDL and nLDL on ABCA1 mRNA and protein expression in THP-1 macrophages
left panel: mRNA expression (n=4, mean± SD, * $p < 0.05$, ** $p < 0.01$, two-way ANOVA), right panel: protein expression (n=3, mean ± SD) and representative Western blot image

Furthermore, ABCA1 protein expression was measured by Western blot analysis in HMDM. HMDM obtained from three healthy adult volunteers were incubated under the same conditions as THP-1 cells. However, when analyzing ABCA1 protein expression, no differences between treatments could be observed and the results were inconsistent with high standard deviations (results not shown). Therefore, it was not possible to confirm the findings obtained in THP-1 macrophages.

5.3.2 Effect of carbamylated and native LDL on ABCG1 expression

Similar to ABCA1 mRNA expression, ABCG1 mRNA was increased when THP-1 cells were incubated with cLDL compared to nLDL as shown in figure 9 (left panel). Here, all cLDL concentrations studied led to a statistically significant increase in ABCG1 mRNA when analyzed by two-way ANOVA. Whereas increasing concentrations of nLDL did not increase ABCG1 mRNA, it was elevated ~1.6 fold at the lowest (12.5 µg/ml) cLDL concentration and slightly increased up to ~1.9 fold when incubated with 100 µg/ml cLDL.

In contrast to the qPCR experiments, Western blot analysis of ABCG1 protein (figure 9, right panel) gave different results. Here, THP-1 macrophages incubated with both, 12.5 µg/ml nLDL or cLDL resulted in a similar protein expression of ABCG1. Contrary to the qPCR results, nLDL seemed also to influence ABCG1 protein expression, as all nLDL concentrations studied increased ABCG1 protein. Nevertheless, cLDL may have a stronger impact on ABCG1 protein expression than nLDL. Incubation with increasing cLDL concentrations increased the expression of ABCG1 stronger as compared to nLDL incubations. In addition, 100 µg/ml cLDL even doubled the amount of ABCG1 protein compared to control samples (BSA incubation). However, the obtained Western blot results were not significant.

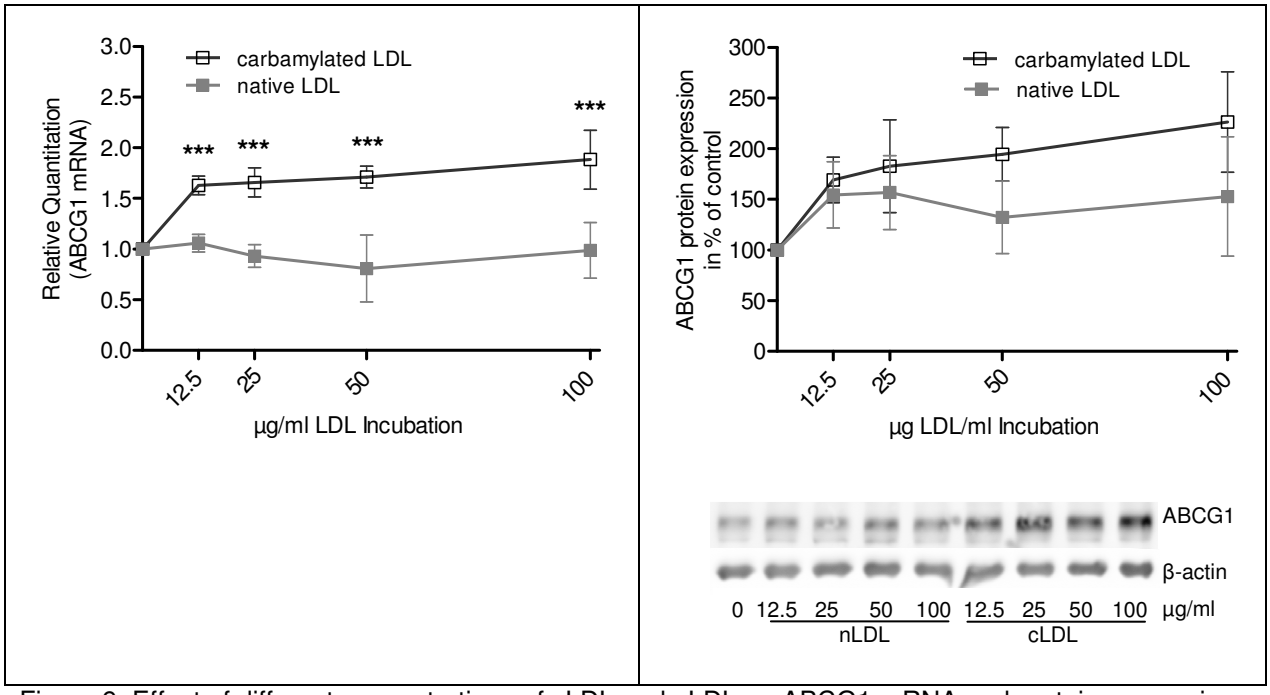

Figure 9: Effect of different concentrations of cLDL and nLDL on ABCG1 mRNA and protein expression in THP-1 macrophages
left panel: mRNA expression (n=4, mean± SD, *** $p < 0.001$, two-way ANOVA), right panel: protein expression (n=3, mean ± SD) and representative Western blot image

ABCG1 protein expression was also measured in HMDM obtained from three healthy volunteers. Cells were incubated under the same conditions as described above. Western blot analysis (not shown) could partly confirm the results achieved with THP-1 macrophages. In contrast to THP-1 macrophages, increasing cLDL concentrations increased ABCG1 protein as compared to nLDL incubation in HMDM. Furthermore, treatment of HMDM with nLDL did not change protein expression. Even though the results had high standard deviations and were not significant, a trend towards increasing ABCG1 protein expression with cLDL incubation could be recognized.

5.3.3 Effect of carbamylated and native LDL on SR-BI expression

THP-1 macrophages showed an increase in SR-BI mRNA when incubated with both, nLDL and cLDL. The effect was analyzed via one-way ANOVA and all LDL incubations increased ($p < 0.001$) SR-BI mRNA compared to control incubation in the absence of LDL. Moreover, this effect did not appear to be dose-dependent and all incubations with the concentrations studied led to a similar result, namely upregulation of SR-BI mRNA.

We observed a different outcome after analyzing SR-BI protein expression by Western blot experiments. Neither nLDL nor cLDL changed the SR-BI protein concentration at lower concentrations (from 12.5 to 50 µg/ml). However, incubations with 100 µg/ml cLDL tended to increase SR-BI protein. This trend, however, was not significant.

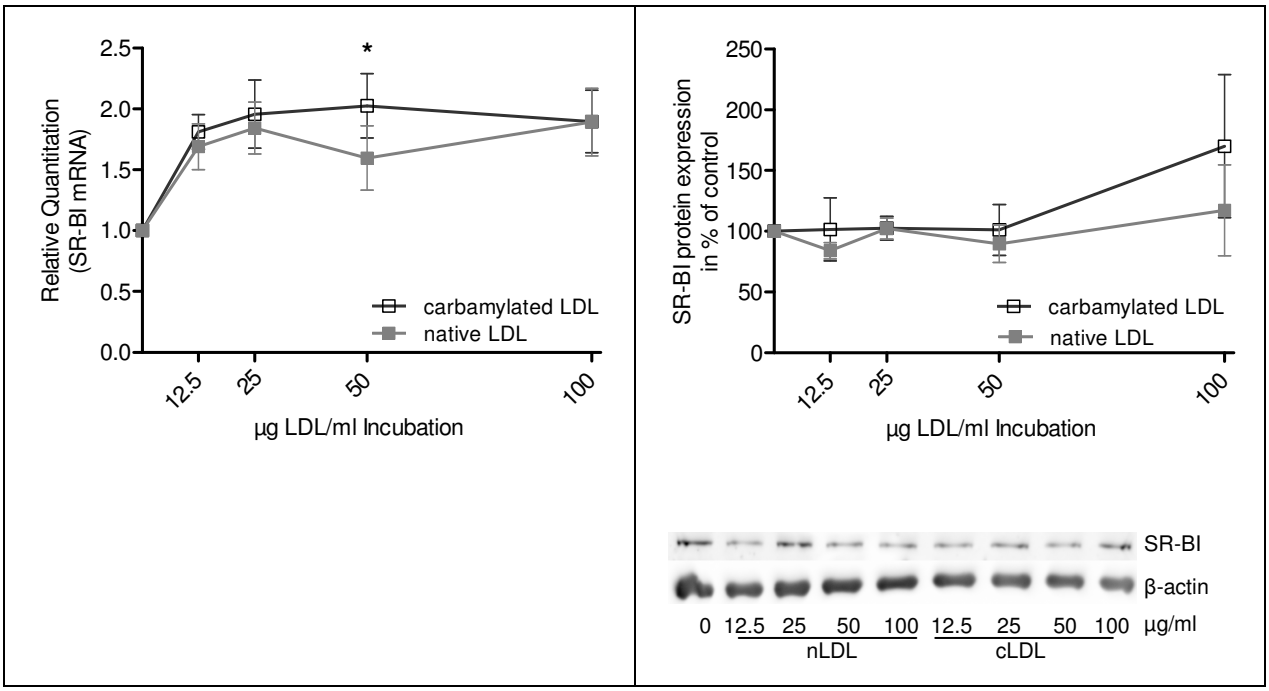

Figure 10: Effect of different concentrations of cLDL and nLDL on SR-BI mRNA and protein expression in THP-1 macrophages
left panel: mRNA expression (n=4, mean± SD, * $p < 0.05$, two-way ANOVA), right panel: protein expression (n=3, mean ± SD) and representative Western blot image

SR-BI protein expression also was measured by Western blot analysis in HMDM incubated with different concentrations of nLDL and cLDL. The results obtained were inconsistent and the different HMDM preparations yielded inconsistent data for SR-BI protein (not shown). The findings obtained in THP-1 macrophages could not be confirmed for that reason.

5.3.4 Effect of carbamylated and native LDL on LXRα expression

LXRα expression was determined on an mRNA level via qPCR. Incubation of THP-1 macrophages with nLDL did not alter LXRα mRNA expression as compared to control (figure 11). Moreover, low doses of cLDL did not change LXRα mRNA as well. We could find a significant effect of cLDL only when THP-1 macrophages were incubated with a high concentration (100 µg/ml). Here, THP-1 macrophages treated with 100 µg/ml cLDL showed a 3-fold increase in LXRα mRNA as compared to control.

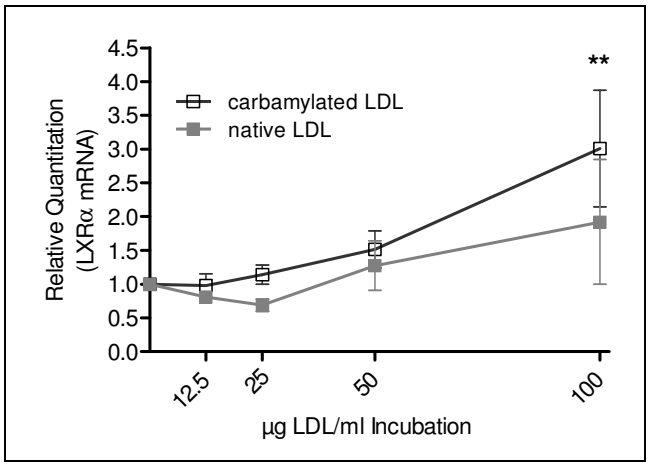

Figure 11: Effect of different concentrations of cLDL and nLDL on LXRα mRNA expression in THP-1 macrophages
(n=4, mean ± SD, ** $p < 0.01$, two-way ANOVA)

5.4 Effect of the LXR antagonist GGPP on ABCA1, ABCG1 and SR-BI protein expression in THP-1 macrophages incubated with cLDL and nLDL

To determine whether the effects of cLDL on ABCA1, ABCG1 and SR-BI are at least in part mediated by LXR, cLDL and nLDL incubated THP-1 macrophages were treated with geranyl-geranyl-pyrophosphate (GGPP) to antagonize LXR (Gan et al., 2001). Therefore, THP-1 macrophages were incubated with 50 µg/ml cLDL or nLDL for 48 hours. BSA (2 mg/ml) incubation was used as control. 10 µM GGPP was added to the cells 24 hours prior to cell lysis.. As GGPP is dissolved in methanol, control incubations without GGPP were performed where cells were treated with the same volume (i.e. 6.76 µl in 1.5 ml medium) of methanol instead of GGPP. After cell lysis, Western blot analysis was performed and the protein expression of BSA treated THP-1 macrophages without GGPP incubation was set to 100 %.

Even though we could observe that GGPP tended to decrease ABCA1 protein to ~80 % of control (BSA incubation), the obtained results were not significant. Furthermore, GGPP did not change ABCA1 protein expression in THP-1 macrophages treated with both, nLDL or cLDL (figure 12).

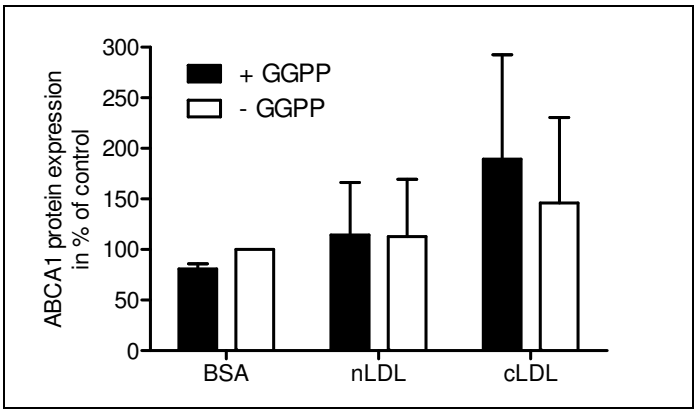

Figure 12: Effect of GGPP on ABCA1 protein expression in THP-1 macrophages (n=2, mean ± SD)

Similarly, Western blot analysis of ABCG1 protein expression (figure 13) of THP-1 macrophages with the same treatments did not show a significant change when cells were incubated with or without GGPP.

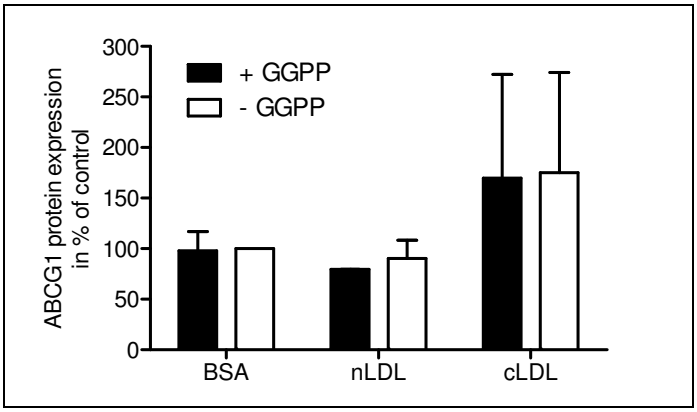

Figure 13: Effect of GGPP on ABCG1 protein expression in THP-1 macrophages (n=2, mean ± SD)

Considering SR-BI, GGPP did not appear to influence its expression as illustrated in figure 14. No differences between incubations with or without GGPP could be observed.

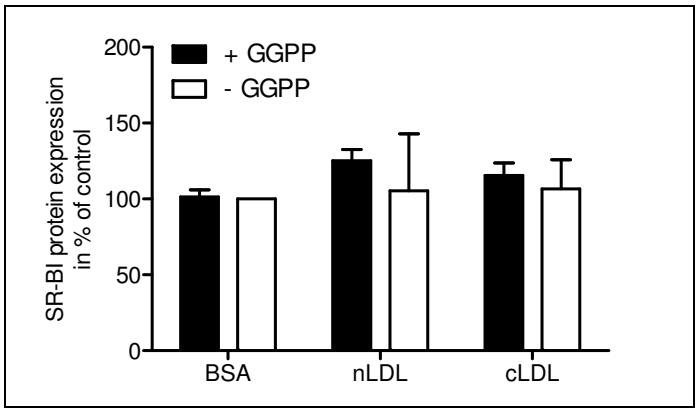

Figure 14: Effect of GGPP on SR-BI protein expression in THP-1 macrophages
(n=2, mean ± SD)

5.5 Effect of blocking ABCA1 by probucol on cholesterol efflux in THP-1 macrophages incubated with cLDL and nLDL

As cLDL induced an increased cholesterol efflux to apoA-I in THP-1 macrophages (cpt. 5.2.1), it was of interest, whether this increase was mediated by ABCA1 and thus, could be inhibited by probucol. Probucol is a substance supposed to inhibit ABCA1-mediated cholesterol efflux by inhibiting the translocation of ABCA1 to the plasma membrane (Favari et al., 2004). For this purpose, cholesterol efflux to apoA-I, HDL and serum from cLDL, nLDL or BSA treated THP-1 macrophages with or without probucol was measured.

Compared to BSA and nLDL incubation of THP-1 macrophages, cLDL increased the cholesterol efflux to apoA-I. However, figure 15 demonstrates that probucol was not able to counteract this effect. Furthermore, probucol had no significant effect on apoA-I-mediated cholesterol efflux in cells incubated with BSA and nLDL.

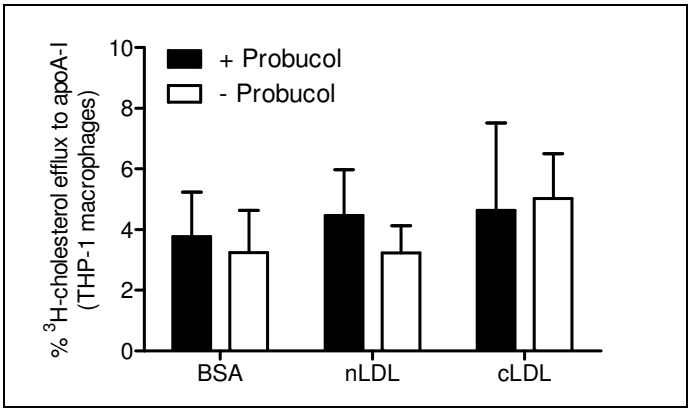

Figure 15: Effect of probucol on cholesterol efflux from THP-1 macrophages incubated with BSA, nLDL or cLDL to apoA-I
Efflux to 10 µg/ml apoA-I (n=4, mean ± SD).

In addition, cholesterol efflux to HDL and serum was measured under the same conditions. The cholesterol efflux to both acceptors was unaltered when cells were exposed to probucol as illustrated in figure 16.

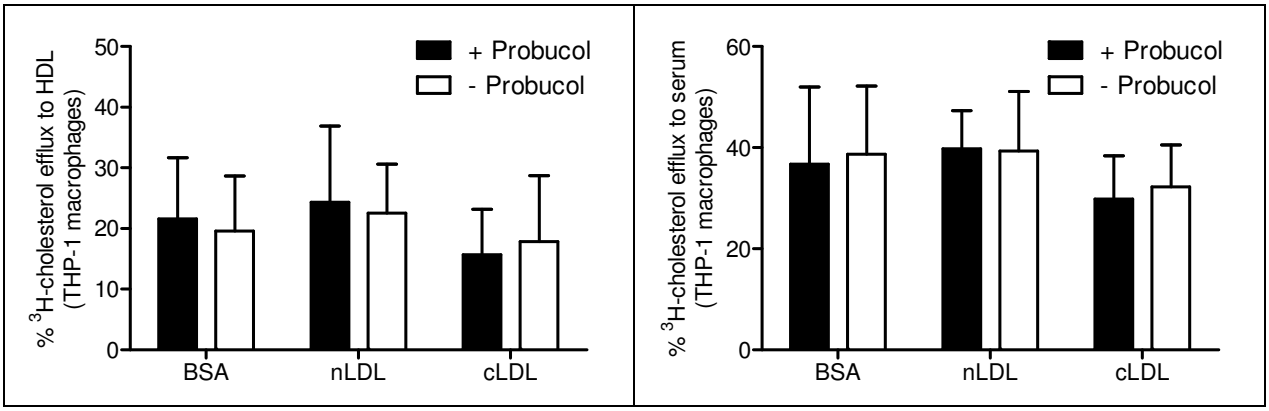

Figure 16: Effect of probucol on cholesterol efflux from THP-1 macrophages incubated with BSA, nLDL or cLDL to serum or HDL
Left panel: efflux to 10 µg/ml HDL, right panel: efflux to 1 % serum (n=4, mean ± SD).

To provide evidence of the effectiveness of probucol in THP-1 macrophages on cholesterol efflux, further experiments using cholesterol loaded cells were performed as originally described by Favari et al., 2004. Macrophages were treated with acLDL to induce extensive intracellular cholesterol accumulation and with a synthetic LXR-agonist to upregulate cholesterol efflux transporters. Control incubations were performed in the absence of LXR-agonist. Cholesterol efflux to apoA-I, HDL or serum was measured after probucol incubation.

Probucol reduced the cholesterol efflux to apoA-I in THP-1 cells only when LXR was stimulated (figure 17, right panel). In cells without LXR-agonist treatment (left panel), probucol had no effect on the efflux to apoA-I. Moreover, cholesterol efflux to HDL and serum was studied under the same conditions. Here, probucol did not influence cholesterol efflux.

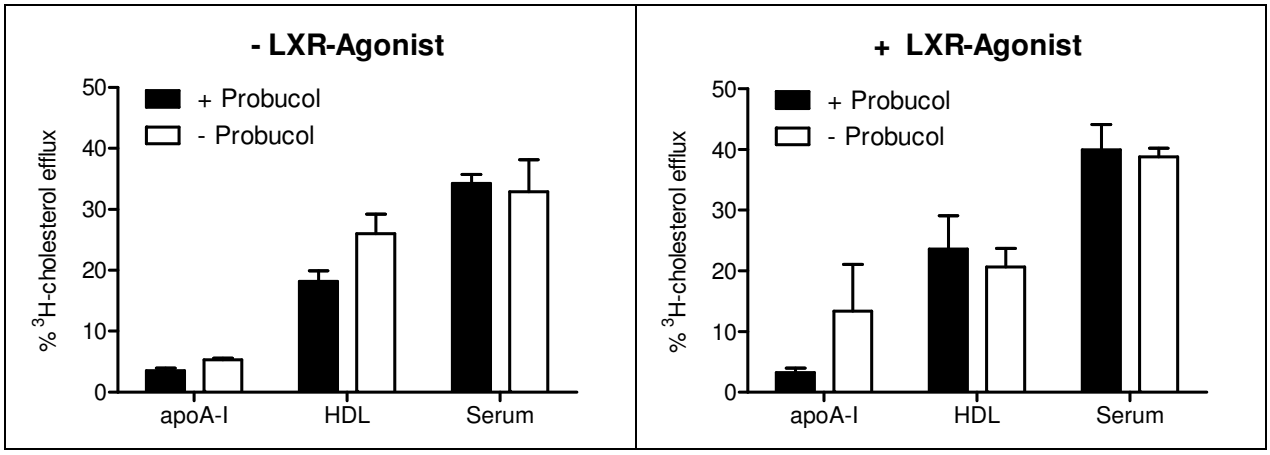

Figure 17: Effect of probucol on cholesterol efflux from acLDL-loaded THP-1 macrophages to apoA-I, HDL and serum
Left panel: cells without LXR-agonist treatment, right panel: cells with LXR-agonist treatment (n=3, mean ± SD).

5.6 Analysis of ABCA1, ABCG1, SR-BI and LXRα during THP-1 differentiation

In differentiated macrophages, LXRα regulates the expression of ABCA1, ABCG1 and SR-BI (Tontonoz et al., 2003; Hu et al., 2010). To determine whether this also occurs during differentiation, we tested whether LXRα mRNA expression correlates with ABCA1, ABCG1 and SR-BI expression during THP-1 differentiation.

For characterization of the change in expression of ABCA1, ABCG1, SR-BI and LXRα during THP-1 differentiation, THP-1 monocytes were differentiated with PMA towards macrophages. RNA and proteins were isolated at day 0, 1, 2 and 3 of differentiation for their further analysis. Day 0 represents the monocytic state and at day 3, THP-1 macrophages were fully differentiated. For evaluation, values obtained on day 0 were set to 100 % for Western blot and to RQ 1 for qPCR results.

5.6.1 ABCA1 mRNA and protein expression during THP-1 differentiation

ABCA1 mRNA expression increased during differentiation as depicted in figure 18. A twofold increase of ABCA1 mRNA could be observed in differentiated THP-1 macrophages (day 3) compared to THP-1 monocytes (day 0). Considering ABCA1 protein expression, the same trend could be noticed and differentiated cells expressed even 2.7 fold more ABCA1 protein than undifferentiated cells.

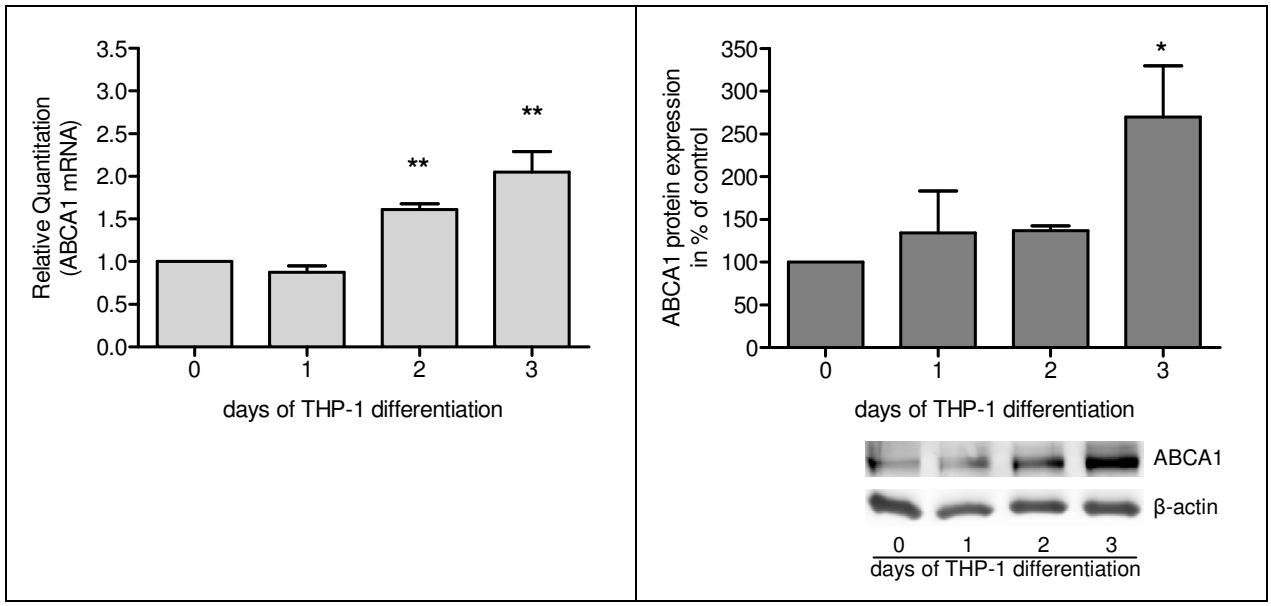

Figure 18: ABCA1 mRNA and protein expression during THP-1 differentiation
left panel: mRNA expression (n=2, mean ± SD, ** $p < 0.01$, one-way ANOVA, compared to day 0), right panel: protein expression (n=2, mean ± SD, * $p < 0.05$, one-way ANOVA, compared to day 0) and representative Western blot image

5.6.2 ABCG1 mRNA and protein expression during THP-1 differentiation

When characterizing ABCG1 expression, both, mRNA and protein (figure 19) did not differ between between differentiated THP-1 macrophages and undifferentiated THP-1 monocytes but a transient decrease of ABCA1 mRNA could be observed on day 1 and day 2 of differentiation. However, ABCG1 protein expression did not change significantly during THP-1 differentiation.

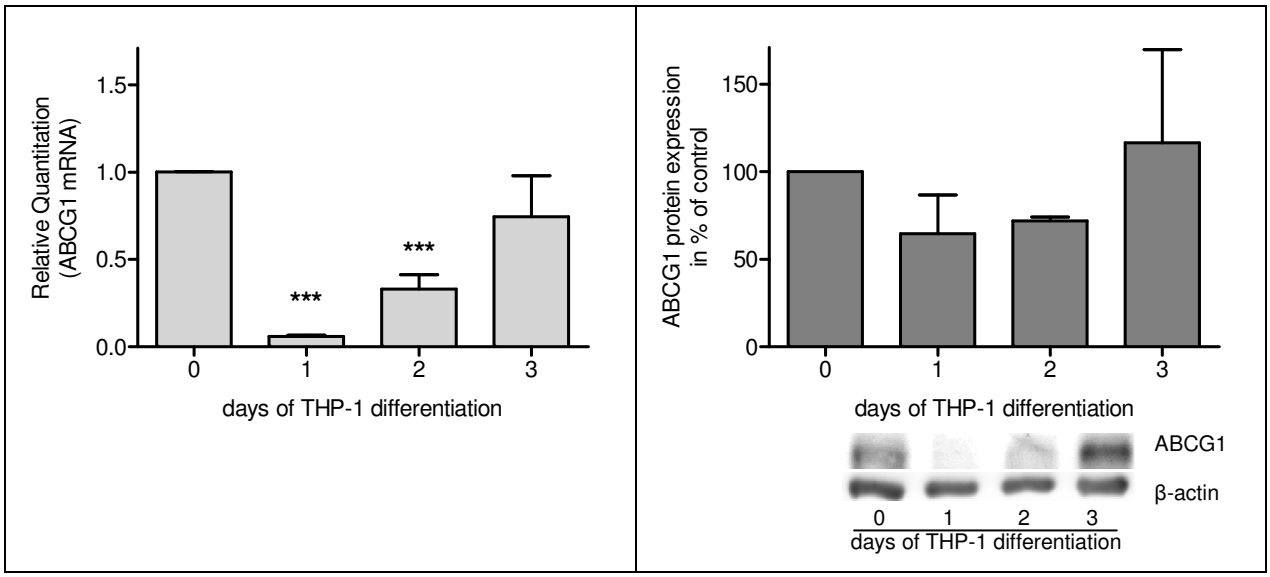

Figure 19: ABCG1 mRNA and protein expression during THP-1 differentiation
left panel: mRNA expression (n=3, mean ± SD, *** $p < 0.01$, one-way ANOVA, compared to day 0), right panel: protein expression (n=2, mean ± SD)

5.6.3 SR-BI mRNA and protein expression during THP-1 differentiation

SR-BI mRNA and protein decreased with proceeding differentiation of THP-1 cells as schematized in figure 20. When comparing mRNA and protein expressed during the different time points with the expression on day 0, a significant change could be noticed. The decrease appeared more pronounced for mRNA than for protein: mRNA was reduced by 86 % whereas protein was decreased by 68 % in differentiated THP-1 macrophages compared to the expression on day 0.

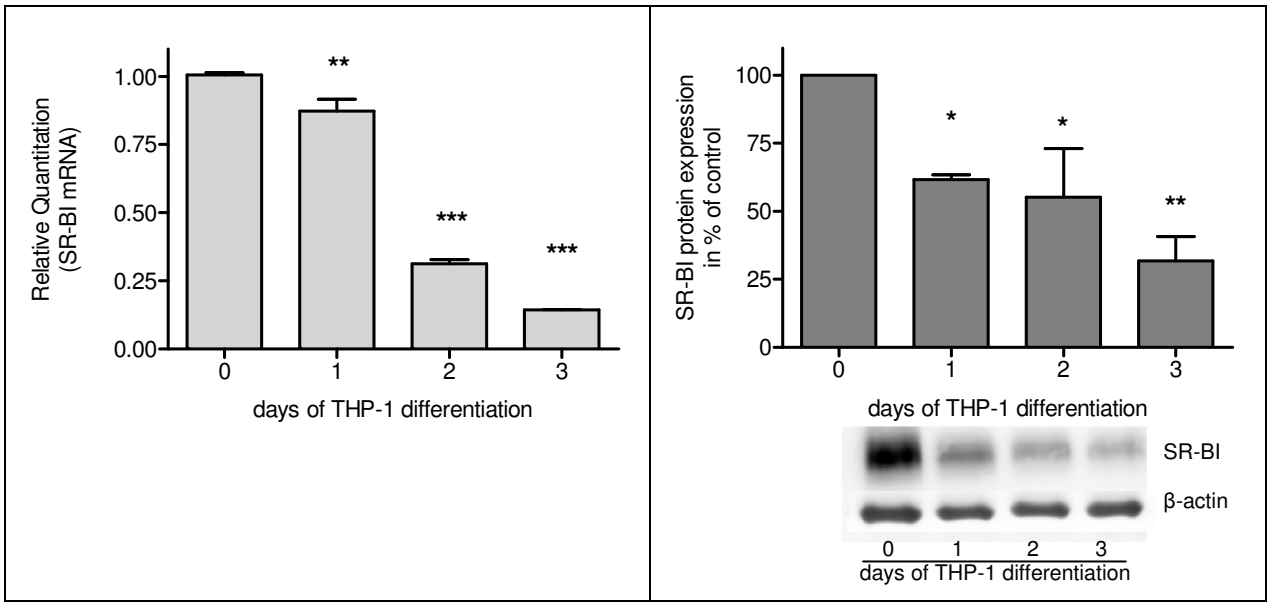

Figure 20: SR-BI mRNA and protein expression during THP-1 differentiation
left panel: mRNA expression, right panel: protein expression (n=2, mean ± SD, * $p < 0.05$, ** $p < 0.01$, *** $p < 0.001$, one-way ANOVA, compared to day 0)

5.6.4 LXRα mRNA expression during THP-1 differentiation

Our results show that the level of LXRα mRNA remained unchanged (figure 21) during THP-1 differentiation and hence, did not correlate with either ABCA1, ABCG1 or SR-BI expression.

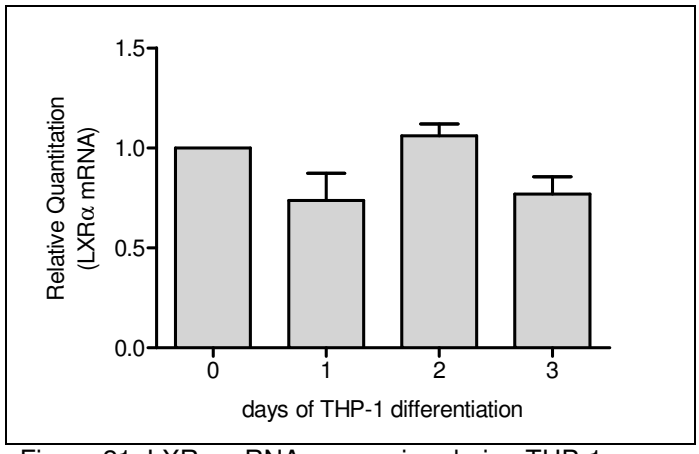

Figure 21: LXRα mRNA expression during THP-1 differentiation
(n=2, mean ± SD)

5.7 Effect of modified LDL on miRNA expression in THP-1 macrophages

THP-1 macrophages showed an increased SR-BI mRNA expression when incubated with both, nLDL and cLDL (cpt. 5.3.3). Therefore, we examined, whether the expression of miR-223, which is predicted to target SR-BI mRNA (Vickers et al., 2011), correlates with these observations. Moreover, we observed that cLDL significantly increased ABCA1 mRNA expression (cpt. 5.3.1) and hence, we hypothesized that miR-33a expression in cells incubated with cLDL may be lowered because miR-33a targets ABCA1 mRNA (Rayner et al., 2010). To address these questions, the expression of miR-223 and miR-33a was measured in THP-1 macrophages incubated with modified forms of LDL (50 µg/ml) for 48 hours. In addition to nLDL and cLDL, also oxLDL and acLDL were used in the incubation experiments to study their influence on miR-223 and miR-33a level in THP-1 macrophages. BSA (2 mg/ml) incubation was used as control.

As illustrated in the left panel of figure 22, both, cLDL and nLDL induced a ~10 % lower expression of miR-223 compared control incubation (BSA), which was set to an RQ value of 1 (represented by the dotted line). Furthermore, miR-223 expression was

increased in oxLDL and acLDL treated cells. However, the changes to control incubations were small and thus, represent rather a trend than a clear effect. The right panel shows miR-33a expression in THP-1 macrophages incubated with modified LDLs. No difference of miR-33a expression could be observed between treatments.

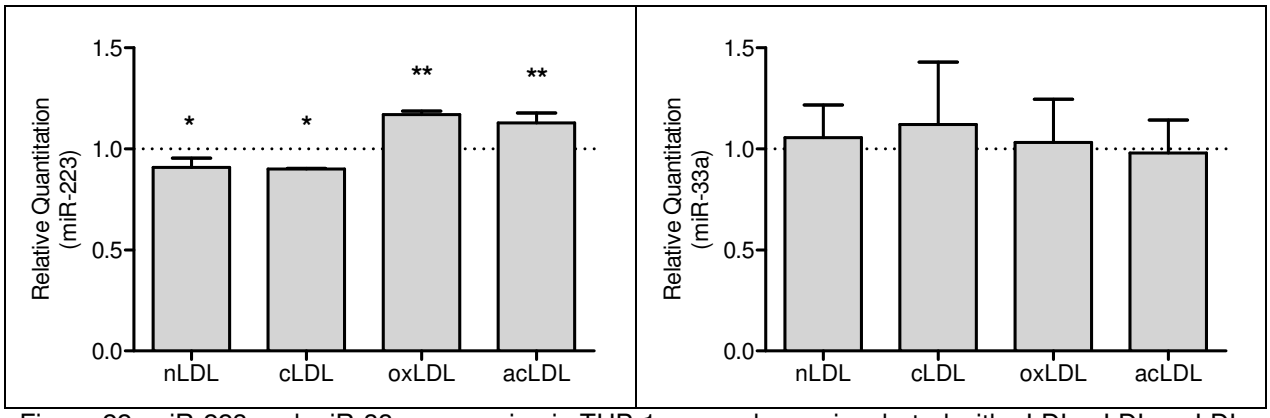

Figure 22: miR-223 and miR-33a expression in THP-1 macrophages incubated with nLDL, cLDL, oxLDL or acLDL
left panel: miR-223 expression (n=2, mean ± SD, * $p < 0.05$, ** $p < 0.01$, one-way ANOVA, compared to control incubation), right panel: miR-33a expression (n=2, mean ± SD); the dotted line represents the expression of the reference sample (BSA incubation) for which the RQ value was set to 1.

5.8 Cholesterol acceptor capacity of cHDL

Increased plasma urea levels, caused by CRF lead to increased carbamylation of proteins (Wang et al., 2007b). Therefore, we asked whether the ability of HDL to accept cholesterol is altered when it is carbamylated.

5.8.1 Capacity of cHDL to accept cellular cholesterol from THP-1 macrophages

Cholesterol efflux from THP-1 macrophages was measured to native HDL and *in vitro* carbamylated HDL with different degrees of carbamylation. To obtain various HDL preparations with different degrees of carbamylation, two different approaches were used. First, different concentrations of KCNO were used in individual carbamylation reactions of HDL. Second, one HDL sample was carbamylated and further diluted stepwise with native HDL to obtain HDL samples with different amounts of carbamylated particles. In both approaches, the highest carbamylated HDL sample was produced with the same concentration of KCNO (246.5 mM). Efflux was measured from cholesterol-loaded (acLDL) THP-1 macrophages treated with an LXR-agonist..

Cholesterol efflux to cHDL did not differ from efflux to nHDL as shown in figure 23, irrespective of the degree of HDL carbamylation. Both cholesterol efflux experiments

with carbamylated HDL samples yielded similar results. Therefore, the cholesterol acceptor capacity of HDL seemed to be independent of its carbamylation status.

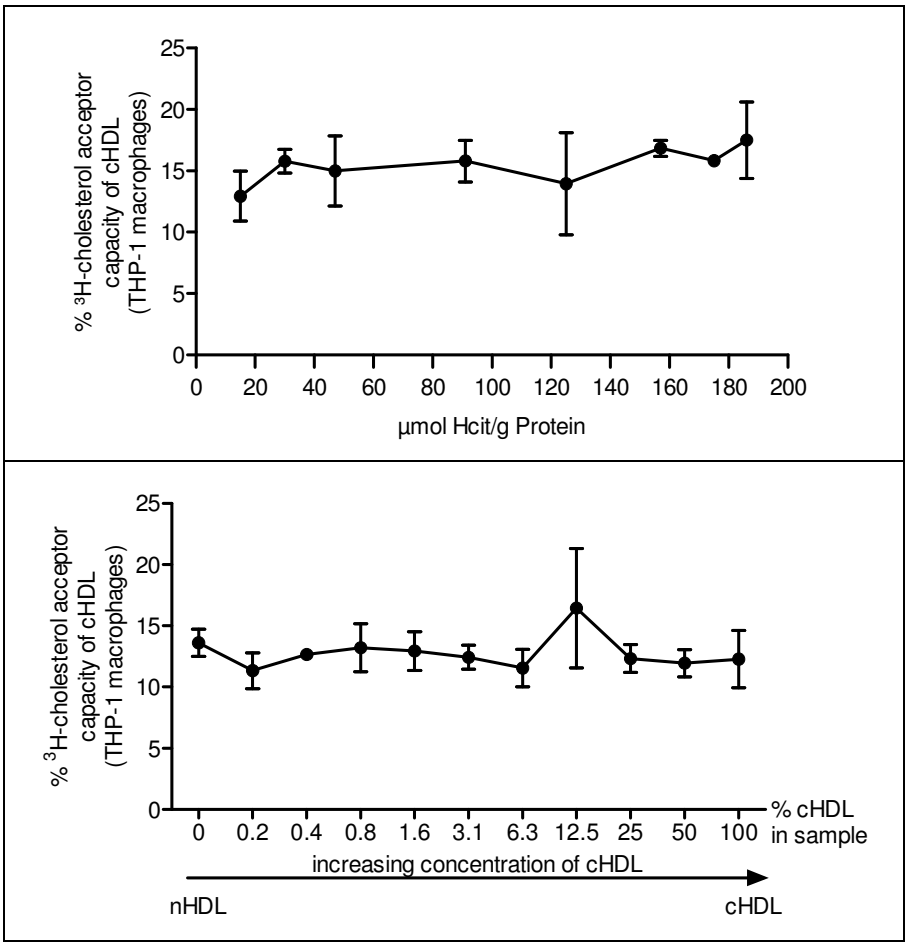

Figure 23: Cholesterol acceptor capacity of cHDL (THP-1 macrophages) top panel: efflux to individually carbamylated HDL samples, (n=2, mean ± SD), values on the x-axis represent measured degrees of carbamylation (cpt.5.1.2); bottom panel: efflux to cHDL, stepwise diluted with nHDL (n=2, mean ± SD)

5.8.2 Capacity of cHDL to accept cellular cholesterol from HMDM

To confirm the results obtained with THP-1 macrophages, cholesterol efflux to cHDL and nHDL from cholesterol-loaded (acLDL) HMDM treated with an LXR-agnoist was measured. In HMDM, the cholesterol efflux capacity of HDL tended to decrease when it was carbamylated (figure 24). However, statistical analysis of the reduced cholesterol acceptor capacity of cHDL using HMDM as cell model reached no significance. Therefore, carbamylation may not impair the cholesterol acceptor capacity of HDL.

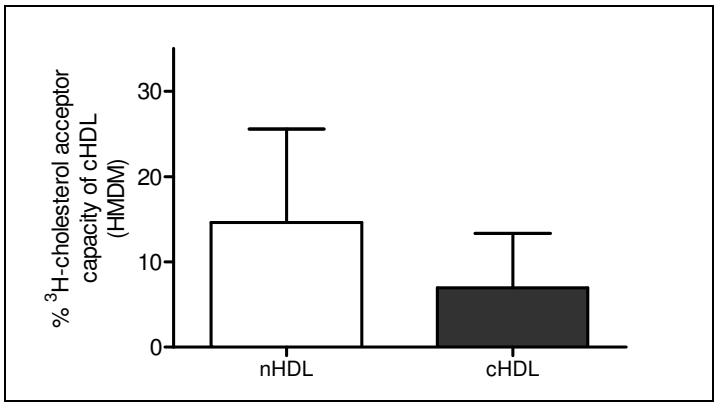

Figure 24: Cholesterol acceptor capacity of cHDL (HMDM)
(n=4, mean ± SD)

5.9 Cholesterol acceptor capacity of serum from CRF- and hemodialysis patients

We studied whether the cholesterol acceptor capacity of serum in renal disease is altered compared to serum of healthy subjects. For this purpose, cholesterol efflux to serum of patients with CRF (n=17) and to serum of patients with ESRD on hemodialysis treatment (n=14) was measured using cholesterol-loaded (acLDL) THP-1 macrophages incubated with an LXR-agonist. Furthermore, efflux was measured to serum from healthy matched individuals (n=17 and n=14, respectively).

The cholesterol acceptor capacity of serum from CRF-patients was significantly ($p < 0.05$) higher than those of healthy controls, albeit this difference (3.5 %) was very small (figure 25, left panel). In contrast, serum of ESRD-patients on hemodialysis treatment had a diminished cholesterol acceptor capacity (5 %) compared to serum of matched controls ($p < 0.001$) as shown in figure 25 (right panel).

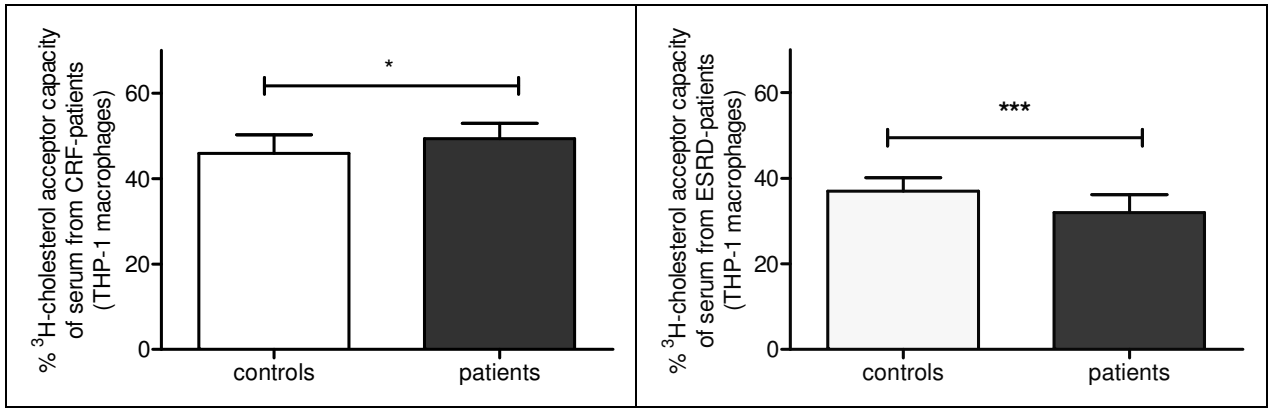

Figure 25: Cholesterol acceptor capacity of serum from CRF- and hemodialysis patients using THP-1 macrophages
left panel: efflux to serum of CRF-patients and matched controls (n=17, mean ± SD, * $p < 0.05$, unpaired t-test), right panel: efflux to serum of ESRD-patients and matched controls (n=14, mean ± SD, *** $p < 0.001$, unpaired t-test)

To confirm the results obtained with THP-1 macrophages, experiments were performed in which cholesterol efflux was measured from acLDL-loaded HMDM treated with an LXR-agonist to pooled serum of patients with CRF and ESRD-patients on hemodialysis treatment and matched controls.

As shown in figure 26, the cholesterol acceptor capacity of pooled serum from both, CRF-patients and ESRD-patients on hemodialysis treatment, did not differ as compared to serum of controls and hence, the results shown in figure 25 could not be confirmed in HMDM.

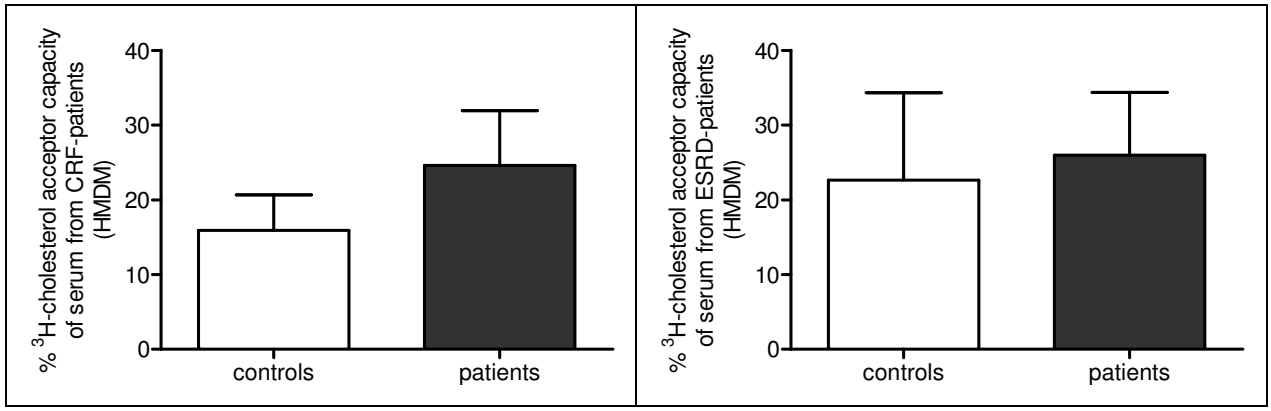

Figure 26: Cholesterol acceptor capacity of serum from CRF- and hemodialysis patients using HMDM
left panel: efflux to pooled serum of CRF-patients and controls (n=4, mean ± SD) right panel: efflux to pooled serum of ESRD-patients and controls (n=4, mean ± SD)

6 Discussion

Patients suffering from CRF are highly susceptible to atherosclerosis. In spite of known risk factors like enhanced oxidative stress, inflammation or dyslipidemia (reviewed by Vaziri et al., 2011) the increased incidence of atherosclerosis in CRF-patients is not fully understood. CRF-patients have elevated levels of plasma urea (Kraus et al., 2001). The active form of cyanate, isocyanic acid, is derived from urea and chemically modifies proteins by carbamylation, thereby altering the structure and functional properties of proteins. The formation of isocyanic acid is promoted by increased blood urea levels as found in patients suffering from CRF (Jaisson et al., 2011). In this context, the apolipoproteins of LDL and HDL are prone to carbamylation (Gonen et al., 1985; Holzer et al., 2011). Furthermore, it has been described that CRF-patients have increased plasma cLDL-levels (Apostolov et al., 2005). It is known, that modified forms of LDL are taken up nonspecifically by arterial macrophages via several scavenger receptors and that this nonspecific uptake leads to the formation of foam cells (for review see Moore et al., 2011). However, the molecular mechanisms underlying the effect of cLDL on macrophages are poorly understood.

In this study, we tried to elucidate the effects of cLDL on human macrophages using THP-1 cells and human monocyte-derived macrophages. LDL isolated from healthy, normolipidemic volunteers was carbamylated *in vitro.* To ensure proper carbamylation, the relative electrophoretic mobility (REM) as well the degree of carbamylation was evaluated. With these measurements we could confirm that LDL was carbamylated appropriately based on the charge alteration of cLDL (REM of 2). Furthermore, a colorimetric assay was performed to measure the degree of carbamylation of LDL. Again, we could confirm appropriate carbamylation of the LDL preparations, which were used throughout further experiments. According to the measurements, cLDL contained ~3.6 fold more protein bound homocitrulline than nLDL.

Carbamylated LDL lacks the ability to bind to the LDL-receptor. In contrast, cLDL is mostly recognized by scavenger receptors (for review see Basnakian et al., 2010), preferably SR-A, and it is taken up in a nonspecific and unregulated manner (Wang et al., 2007b). We studied the effect of cLDL on the cholesterol efflux capacity of human macrophages. There was no significant difference in cholesterol efflux to serum or

HDL after incubation with cLDL compared to nLDL. However, a significant increase in cholesterol efflux to apoA-I could be observed when THP-1 macrophages were treated with cLDL compared to nLDL. Cholesterol efflux to apoA-I is mediated by ABCA1 and indeed, ABCA1 mRNA was increased in the presence of cLDL as discussed below. This could explain the elevated cholesterol efflux to apoA-I from cLDL treated THP-1 macrophages. Even so, the cholesterol efflux to apoA-I represents ~10 % of the total cholesterol efflux to serum, which contains a wide spectrum of cholesterol acceptors such as lipoproteins and apolipoproteins. In an attempt to confirm the results obtained with THP-1 cells, LDL incubations and cholesterol efflux experiments were performed under the same conditions using human monocyte-derived macrophages (HMDM). With HMDM, however, it was not possible to obtain significant results due to high standard deviations. Anyhow, a trend towards an increased cholesterol efflux from HMDM to apoA-I was found after cLDL incubation as compared to nLDL. The elevated cholesterol efflux to apoA-I after cLDL-treatment prompted us to further investigate several efflux transporters of macrophages on the mRNA and protein level, and to ask, whether there are any dose-dependent effects of nLDL or cLDL on the expression of these transporters.

Quantitative real-time PCR experiments showed, that ABCA1 and ABCG1 mRNA expression of nLDL-treated THP-1 macrophages was unaltered compared to control incubation (without LDL). Neither the lowest (i.e. 12.5 µg/ml) nor the highest (i.e. 100 µg/ml) nLDL concentration studied altered the mRNA expression of these ABC transporters. Our findings differ from those of some other groups. The studies of Zhu et al., 2005, and Chen et al., 2011, resulted in an increase of ABCA1 expression when macrophages were treated with nLDL. However, Chen and his group did not use human but mouse macrophages and the group of Zhu incubated THP-1 macrophages with 1.8 mg/ml nLDL and found a small increase in ABCA1 mRNA. The highest concentration we have used in our experiments was much lower, namely 100 µg/ml. In contrast to the results obtained with nLDL, we could show that cLDL-treated THP-1 macrophages had elevated levels of ABCA1 and ABCG1 mRNA even when cells were incubated with low (12.5 µg/ml) cLDL concentrations. Furthermore, the mRNA levels significantly increased with increasing cLDL concentrations. Western blot experiments were performed to measure ABCA1 and ABCG1 protein expression from THP-1 macrophages treated with different concentrations of nLDL or cLDL. These

experiments produced no significant results due to high standard deviations, but also here, a clear trend towards an increase of ABCA1 and ABCG1 protein expression was found. nLDL did not appear to influence ABCA1 protein expression. Contrary to the qPCR results, nLDL incubation resulted in an increase of ABCG1 protein expression, even though the effect was not as strong as the cLDL-induced elevation. ABCA1 and ABCG1 protein expression was also measured in cLDL and nLDL-treated HMDM, but the experiments did not produce significant differences. However, in these cells too, we could find a trend towards a cLDL-induced elevation of the protein levels of ABCA1 and ABCG1.

The receptor SR-BI, which is located in the plasma membrane, is highly expressed in the liver. There, it mediates the terminal step of RCT, namely uptake of HDL cholesterol. Beyond that, SR-BI is also expressed in macrophages and it is supposed to be involved in the cholesterol efflux from these cells (for review see Moore et al., 2006). However, the role of SR-BI in the first part of RCT is not well defined and the findings of several studies are controversial. The group of Wang demonstrated, that SR-BI is not involved in macrophage RCT in mice *in vivo* (Wang et al., 2007a). They proposed that primarily ABCA1 and ABCG1 contribute to this mechanism. In contrast, Zhao et al., 2010, showed that in ABCA1/SR-BI double knockout mice macrophage foam cell formation is enhanced as compared to single knockout mice, indicating that SR-BI and ABCA1 act synergistically to regulate cholesterol homeostasis in macrophages in mice *in vivo*.

Hirano et al., 1999, demonstrated that SR-BI mRNA and protein is increased in HMDM after acLDL or oxLDL incubation. To determine the role of cLDL on SR-BI macrophage RCT, we aimed to identify, whether incubation with cLDL alters the expression of SR-BI in human macrophages. Therefore, we determined the mRNA and protein expression of SR-BI in cLDL- and nLDL-incubated THP-1 macrophages. In our experiments, the SR-BI mRNA level doubled when cells were incubated with either nLDL or cLDL compared to incubation without LDL. Hence, these results suggest that LDL in general, irrespective of whether it is carbamylated or not, increases SR-BI mRNA. We could not find any dose-dependent effects of cLDL and nLDL on SR-BI expression as there was no difference in the mRNA levels between low-dose (12.5 µg/ml) and high-dose (100 µg/ml) treatments. In contrast, the results obtained from Western blot experiments were different. Here, the SR-BI protein concentration

was slightly increased when cells were incubated with 100 µg/ml cLDL or nLDL, while incubations with lower doses of cLDL or nLDL did not alter SR-BI protein. SR-BI protein levels do not always correlate with those of SR-BI mRNA (Stangl et al., 2002), which may indicate that SR-BI is highly regulated on a translational or post-translational level.

The nuclear receptor LXRα is involved in the control of cellular lipid homeostasis. LXRs act as cholesterol sensors in cells and regulate the expression of several genes involved in the efflux of cholesterol (Tontonoz et al., 2003). It is commonly accepted, that LXR activation increases ABCA1 (Schwartz et al., 2000; Venkateswaran et al., 2000) and ABCG1 gene expression (Wang et al., 2006), but its role on SR-BI expression is controversial. Several authors identified LXR as an important regulator of SR-BI in their studies (Malerod et al., 2002; Hu et al., 2010), while others do not support this idea (Yu et al., 2004; Bultel et al., 2008). We studied the mRNA expression of LXRα from cLDL- and nLDL-treated THP-1 macrophages to find a possible link to the cLDL-induced elevation of ABCA1 and ABCG1 mRNA and the LDL-induced increase in SR-BI mRNA. In fact, LXRα mRNA expression increased when cells were incubated with increasing concentrations of both, cLDL and nLDL. However, cLDL incubation significantly increased LXRα mRNA compared to nLDL incubation only in THP-1 macrophages incubated with high concentrations of LDL (100 µg/ml). According to these results it appeared possible, that LXRα is involved in the cLDL-induced elevation of ABCA1 and ABCG1 expression. In order to test this hyposthesis, we measured ABCA1, ABCG1 and SR-BI protein expression in THP-1 macrophages which were preincubated with an LXR-antagonist (GGPP). We did not see an effect of GGPP on the cLDL-mediated expression of the proteins studied and therefore it is likely, that not only LXRα but also other factors mediate their regulation.

Favari et al., 2004, demonstrated that probucol inhibits ABCA1-mediated lipid efflux. Since our research showed, that cLDL-treated macrophages had an increased cholesterol efflux to apoA-I compared to nLDL-treated cells, we tried to antagonize this effect by blocking ABCA1 with probucol. In addition, we studied, whether probucol impairs the cholesterol efflux to HDL or serum. However, in our experiments, we could not detect any effect of probucol on cholesterol efflux, neither to apoA-I nor to HDL or serum. In order to demonstrate that our probucol preparation was active, we evaluated its effect on cholesterol-loaded (acLDL) THP-1 macrophages. Here, probucol

effectively lowered the cholesterol efflux to apoA-I, but only when LXR was activated using a synthetic LXR-agonist. Compared to the effect of the LXR-agonist, which elevates the cholesterol efflux to apoA-I from 5 % to 13 %, the effect of cLDL is much smaller (from 2 % to 5 %). Hence, the cLDL-induced raise of the ABCA1-mediated cholesterol efflux may not be robust enough to be inhibited by probucol in a noticeable manner.

Even though we could show in THP-1 macrophages, that cLDL enhances apoA-I-mediated cholesterol efflux and it upregulates several cholesterol efflux transporters, this mechanisms do not seem to counteract the imbalance between cholesterol influx and efflux of cholesterol because cLDL induces foam cell formation as we have observed under the microscope (not shown).

It is commonly accepted, that LXRα is an important regulator of the gene expression of ABCA1, ABCG1 (reviewed by Tall, 2008) and possibly SR-BI (Malerod et al., 2002; Hu et al., 2010). Furthermore, it is known that ABCA1 mRNA expression increases during macrophage differentiation (Kielar et al., 2001; Langmann et al., 2003). Thus, we hypothesized that the mRNA expression of LXRα may correlate with that of ABCA1, ABCG1 and SR-BI during THP-1 differentiation. Therefore, we characterized the expression of ABCA1, ABCG1, SR-BI and LXRα during THP-1 differentiation by qPCR experiments. Whereas the LXRα expression remained unchanged during THP-1 differentiation, we could clearly demonstrate, that ABCA1 expression increases with proceeding differentiation. This may indicate that the upregulation of ABCA1 in this situation is independent of LXRα expression. In contrast, the ABCG1 expression on day 0 was similar to the expression on day 3 and on the days between, ABCG1 was downregulated. The reason for the downregulation of ABCG1 on day 1 and day 2 is unclear. It might be due to e.g. a direct action of PMA, the substance used for *in vitro* differentiation (Tsuchiya et al., 1982). We also investigated the SR-BI expression under the same conditions. Our studies showed that SR-BI expression decreased during differentiation. This finding supported those of Murao et al., 1997, who also found decreasing levels of SR-BI during THP-1 differentiation. However, Hirano et al., 1999, studied the SR-BI expression during the differentiation of HMDM, without the use of PMA, and their results indicated an increase in SR-BI expression with proceeding differentiation. An explanation for this contradictory results is lacking but

since PMA is not an endogenous molecule for differentiation initiation, it may induce signal transduction cascades which differ from those during *in vivo* differentiation.

The expression levels of ABCA1, ABCG1 and SR-BI were altered when cells were incubated with cLDL as compared to control. However, cLDL incubation did not induce an increase in LXRα mRNA. Thus, it is likely, that other factors may predominate the regulation of these proteins. Among the possible candidates, we studied the expression of two particular miRNAs, which negatively regulate ABCA1 and SR-BI. MiR-33a is predicted to target ABCA1 mRNA and thereby lowers its expression (Rayner et al., 2010). However, our hypothesis that the cLDL-induced elevation of ABCA1 might be due to a decreased miR-33a expression level could not be confirmed by our experiments. Moreover, the other modified LDLs studied (i.e. acLDL and oxLDL), did not alter miR-33a expression either compared to the control incubation (BSA). In conclusion, we were not able to show in our experiments, that miR-33a expression correlates with the cLDL-induced increase of ABCA mRNA. We also asked, whether the expression of miR-223, which is predicted to target SR-BI mRNA (Vickers et al., 2011), correlates with the elevated SR-BI mRNA expression in nLDL- and cLDL-incubated cells. In fact, our results showed that miR-223 was lowered by about 10 % ($p < 0.05$) compared to control when cells were incubated with nLDL or cLDL. This observation might suggest, that native and also carbamylated LDL may negatively regulate miR-223 expression and thereby indirectly upregulate SR-BI mRNA. In addition, we could show, that acLDL and oxLDL increase miR-223 expression by about 15 % ($p < 0.01$). Several studies indicate, that acLDL and oxLDL incubations reduce SR-BI expression in macrophages (Lam et al., 2004; Yu et al., 2004) and with our results, we further hypothesize, that the increased miR-223 expression may be involved in this effect of both modified LDLs.

Another aim of our study was to determine the cholesterol acceptor capacity of *in vitro* carbamylated HDL compared to native HDL. HDL from healthy, normolipidemic volunteers was carbamylated *in vitro* and similar to cLDL, quality control experiments were performed. The electrophoretic mobility of HDL increased when it was carbamylated and the colorimetric assay using diacetyl monoxime further provided evidence for protein-bound Hcit on the carbamylated HDL samples. cHDL contained ~12 fold more bound Hcit than nHDL. Compared to the results obtained for the cLDL samples, the same amount of KCNO (245.6 mM) used for carbamylation produced

different degrees of carbamylation: 75 µmol Hcit/g protein for cLDL and 190 µmol Hcit/g protein for cHDL, respectively. A possible explanation for this difference may be the different protein composition of these two lipoproteins and the accessibility of their lysines to carbamylation. The only protein component of LDL is one molecule of apoB-100 (as reviewed by Segrest et al., 2001), and the main apolipoprotein HDL is apoA-I (as reviewed by Thomas et al., 2008), both differing considerably in their structure, composition and function. ApoB-100 consists of 4563 amino acids, among them 356 lysines (Chen et al., 1986) . In contrast, apoA-I is a much smaller protein with a primary structure of 243 amino acids and 21 lysine residues (Brouillette et al., 2001). Hence, both proteins contain a similar lysine content (~8 % lysines) and with this information, the higher degree of carbamylation of cHDL compared to cLDL can not be explained and remains unclear.

Patients with CRF have increased plasma urea levels, which lead to carbamylation of proteins (Wang et al., 2007b). The apolipoproteins of HDL are susceptible to this modification (Holzer et al., 2011), but it is not well studied, whether carbamylation alters the cholesterol acceptor capacity of cHDL. Hence, we studied the cholesterol acceptor capacity of carbamylated HDL by measuring cholesterol efflux from cholesterol-loaded THP-1 macrophages, incubated with a synthetic LXR-agonist, to nHDL and to HDL samples with increasing degrees of carbamylation. Our results indicated, that the cholesterol acceptor capacity of HDL seems to be independent of its degree of carbamylation (from 15 to 186 µmol Hcit/g protein). Holzer and his group showed in their publication, that the cholesterol efflux to carbamylated HDL is reduced in THP-1 macrophages infected with an adenovirus encoding SR-BI (Holzer et al., 2011). Cholesterol efflux from control THP-1 macrophages to HDL, however, was unaltered when HDL was carbamylated, which is consistent with our study. In addition, we performed cholesterol efflux experiments using HMDM to confirm the results obtained with THP-1 cells. Here, we observed a slight trend of cHDL towards a lower cholesterol acceptor capacity compared to its native form, but the results were not significant.

Finally, we investigated the cholesterol acceptor capacity of serum obtained from patients with CRF or from patients with ESRD on hemodialysis treatment and respective healthy controls. Cholesterol efflux was measured from cholesterol-loaded THP-1 macrophages treated with an LXR-agonist. Here, we could show that serum

from CRF-patients had a higher cholesterol acceptor capacity than control serum, even though the difference was very small (45 % vs. 49 % cholesterol acceptor capacity). In contrast, serum from ESRD-patients on hemodialysis treatment featured a diminished cholesterol acceptor capacity compared to the respective control serum and this difference was highly significant. ESRD-patients on hemodialysis treatment had significantly lower apoA-I as well as HDL levels compared to their controls (see supplementary data), which may explain the reduced cholesterol acceptor capacity of their serum.

In conclusion, the nonspecific and excessive uptake of carbamylated LDL by macrophages may be compensated in some extent by the upregulation of several cholesterol efflux transporters. We could not demonstrate, that carbamylated HDL had an altered cholesterol acceptor capacity and thus, cHDL may have a minor role in the pathogenesis of atherosclerosis. Nevertheless, the mechanisms by which carbamylated LDL alter gene expression are still unknown and further investigations are needed.

7 Summary

Atherosclerosis is characterized by atheromatous plaques in the arterial wall that may lead to medical complications such as myocardial infarction or stroke. Accelerated atherosclerosis is often found in patients with chronic renal failure (CRF). In addition to the traditional risk factors for atherosclerosis, CRF-patients have elevated plasma urea concentrations, which induce the carbamylation of proteins (such as LDL). Carbamylated LDL (cLDL) is taken up by macrophages in a nonspecific and unregulated way via scavenger receptors, which leads to an enhanced formation of foam cells.

In this study, we asked whether macrophages can compensate for the increased nonspecific uptake of cLDL by increasing cellular cholesterol efflux. Therefore, we investigated cLDL-induced changes in macrophage cholesterol efflux and in the expression of the transporters mediating this efflux process. We could demonstrate that THP-1 macrophages increased the ABCA1-mediated cholesterol efflux to apoA-I when they were exposed to cLDL. We could further show, that cLDL induced an upregulation of ABCA1, ABCG1, SR-BI and, at higher doses, LXRα in THP-1 macrophages. Moreover, native LDL also induced an increase in SR-BI and LXRα expression. To test whether the cLDL-induced change of ABCA1, ABCG1 and SR-BI expression is mediated via LXRα, we treated THP-1 macrophages, which were incubated with BSA, nLDL or cLDL, with an LXR-antagonist (GGPP). We were not able to show a difference in the protein expression of ABCA1, ABCG1 and SR-BI with or without GGPP-treatment. Thus, we assume that besides LXRα, also other factors may be involved in the regulation of the respective genes.

Next, we asked, whether the cLDL-induced increase of the cholesterol efflux to apoA-I could be inhibited by probucol, a substance reported to inhibit ABCA1-mediated cholesterol efflux. The cholesterol efflux to apoA-I of probucol-treated THP-1 macrophages incubated with cLDL did not differ from those without probucol treatment. Probucol, however, reduced the large increase in cholesterol efflux to apoA-I observed in cholesterol-loaded THP-1 macrophages treated with a synthetic LXR-agonist. It appears possible that the cLDL-induced increase of cholesterol efflux to apoA-I was too small to demonstrate the effect of the inhibitor.

In addition, we asked whether LXRα regulates the expression of ABCA1, ABCG1 and SR-BI not only in mature macrophages but also during THP-1 differentiation. We could not find any correlation between the mRNA expression of LXRα and ABCA1, ABCG1 or SR-BI. Thus, we assume that LXRα is not involved in the expression of these genes during macrophage differentiation.

To identify additional factors, which may be involved in the regulation of ABCA1, ABCG1 and SR-BI by modified LDL in mature macrophages, we studied the expression of two candidate microRNAs that are supposed to negatively regulate ABCA1 and SR-BI. The expression of miR-33a, which is predicted to target ABCA1, did not differ between THP-1 macrophages incubated with modified forms of LDL. By contrast, the expression of miR-223, which is predicted to target SR-BI, was decreased slightly when cells were incubated with both, nLDL or cLDL. This is consistent with our results showing that SR-BI mRNA expression was upregulated upon nLDL or cLDL incubation. Furthermore, miR-223 expression was decreased when THP-1 macrophages were incubated with oxLDL or acLDL, two modified LDLs that have been reported to reduce SR-BI mRNA.

Recent data show, that besides LDL, also HDL undergoes carbamylation in patients with CRF and it was suggested that this modification renders HDL dysfunctional. Therefore we studied the effect of *in vitro* carbamylation on HDL cholesterol acceptor capacity (CAC). Even after extensive carbamylation, we could not find any difference in the CAC between native or carbamylated HDL.

The serum levels of cholesterol acceptors are often altered in CRF patients as compared to healthy individuals. Thus, we studied the CAC of serum of these patients and matched healthy controls. Indeed, we found a significant reduction of the CAC of serum of ESRD-patients on hemodialysis treatment, which could be explained in part by low serum apoA-I. Serum of CRF patients in earlier stages of the disease and without hemodialysis, however, had a slightly increased CAC as compared to controls.

In conclusion, we could demonstrate that cLDL alters the gene expression of ABCA1, ABCG1 and SR-BI and thus, changes the cholesterol efflux of THP-1 macrophages. Furthermore, this effect may in part be mediated by LXRα but other molecules, such as microRNAs, may contribute. Thus, the molecular mechanisms behind the cLDL-induced changes remain incompletely understood and need further investigation.

8 Zusammenfassung

Atherosklerose ist durch Ablagerungen in der arteriellen Gefäßwand gekennzeichnet, welche zu medizinischen Komplikationen wie Herzinfarkt oder Schlaganfall führen können. Bei Patienten mit chronischem Nierenversagen (CRF) wird oft ein sehr rascher Verlauf der Atherosklerose beobachtet. Zusätzlich zu den traditionellen Risikofaktoren, weisen CRF-Patienten erhöhte Harnstoffkonzentrationen im Plasma auf, wodurch die Carbamylierung von Proteinen (wie zB LDL) induziert wird. Carbamyliertes LDL (cLDL) wird unspezifisch und unreguliert in Makrophagen aufgenommen, was folglich zur vermehrten Bildung von Schaumzellen führt.

Diese Studie beschäftigt sich mit der Frage, ob dieser erhöhten unspezifischen Aufnahme von cLDL durch eine Erhöhung des zellulären Cholesterinefflux entgegenwirkt wird. Dazu untersuchten wir cLDL-induzierte Veränderungen im Cholesterinefflux von Makrophagen und in der Expression der Transporter, die den Effluxprozess vermitteln. Wir konnten nachweisen, dass Inkubation mit cLDL den Cholesterinefflux aus THP-1 Makrophagen zu apoA-I erhöhte. Wir konnten auch zeigen, dass cLDL die Expression von ABCA1, ABCG1, SR-BI, und bei höheren Dosen auch von LXRα, steigert. Weiters verursachte auch natives LDL (nLDL) einen Anstieg der SR-BI und LXRα mRNA. Um zu untersuchen, ob die von cLDL hervorgerufene Veränderung der Expression von ABCA1, ABCG1 und SR-BI durch LXRα vermittelt wird, inkubierten wir THP-1 Makrophagen mit BSA, nLDL oder cLDL, und mit einem LXR-Antagonisten (GGPP). Im Vergleich zur Kontrollinkubation konnten wir keinen Effekt von GGPP auf die Proteinexpression dieser Transporter feststellen. Somit nehmen wir an, dass neben LXRα auch andere Faktoren an der Regulation der entsprechenden Gene beteiligt sind.

Wir untersuchten, ob die durch cLDL induzierte Steigerung des Cholesterineffluxes zu apoA-I durch Probucol (verhindert den Cholesterinefflux über ABCA1) verhindert werden kann. Dies war jedoch nicht der Fall. Dennoch war es mit Probucol möglich, den starken Anstieg des Cholesterinefflux zu apoA-I in cholesterinbeladenen und mit einem LXR-Agonisten behandelten THP-1 Makrophagen zu reduzieren. Es erscheint möglich, dass die Steigerung des Cholesterineffluxes von cLDL-inkubierten Zellen zu apoA-I zu gering ist um den Effekt des Inhibitors zu erkennen.

Wir prüften, ob LXRα die Expression von ABCA1, ABCG1 und SR-BI nicht nur in reifen Makrophagen, sondern auch während deren Differenzierung reguliert. Wir konnten jedoch keine Korrelation zwischen der mRNA Expression von LXRα und jener von ABCA1, ABCG1 oder SR-BI finden. Somit nehmen wir an, dass LXRα nicht an der Expression dieser Gene während der Makrophagendifferenzierung beteiligt ist.

Um weitere Faktoren zu identifizieren, die an der Regulierung von ABCA1, ABCG1 und SR-BI durch modifizierte LDL in reifen Makrophagen beteiligt sein könnten, untersuchten wir die Expression von miR-33a und miR-223, welche ABCA1 bzw. SR-BI negativ regulieren. In der Expression von miR-33a konnte kein Unterschied im Vergleich zur Kontrolle festgestellt werden, wenn Zellen mit modifizierten Formen von LDL inkubiert wurden. Im Gegensatz dazu verringerte sich miR-223, dessen mögliches Ziel SR-BI ist, in nLDL- oder cLDL-inkubierten THP-1 Makrophagen. Dieser Effekt korreliert damit, dass die SR-BI mRNA durch cLDL bzw. nLDL hochreguliert wurde. Zudem verringerte sich die Expression von miR-223 in oxLDL- oder acLDL-inkubierten Zellen. Beides sind modifizierte Formen von LDL, die die SR-BI mRNA reduzieren.

Neuere Studien zeigten, dass bei CRF-Patienten neben LDL auch HDL carbamyliert wird und dass diese Modifizierung mit einem Verlust der HDL-Funktion einhergehen könnte. Aus diesem Grund untersuchten wir den Effekt von *in vitro* carbamyliertem HDL auf die Cholesterinakzeptorkapazität (CAC). Trotz extensiver Carbamylierung konnten wir keinen Unterschied in der CAC zwischen cHDL und nHDL nachweisen. Weiters sind die Cholesterinakzeptoren im Serum von CRF-Patienten häufig verändert. Tatsächlich konnten wir eine signifikante Reduktion der CAC von Seren von Dialysepatienten finden. Diese konnte zum Teil durch deren geringen Anteil von apoA-I im Serum erklärt werden. Serum von CRF-Patienten, die noch keine Dialyse benötigen, hatte hingegen eine gering erhöhte CAC.

Mit unserer Studie konnten wir zeigen, dass cLDL die Genexpression von ABCA1, ABCG1 und SR-BI, und in weiterer Folge den Cholesterinefflux aus Makrophagen verändert. Die molekularen Mechanismen der cLDL-vermittelten Veränderungen sind jedoch nicht vollständig geklärt und weitere Untersuchungen sind notwendig, um die Rolle von cLDL in der Entstehung von Atherosklerose aufzuklären.

9 References

Ambros, V. (2004). The functions of animal microRNAs. *Nature, 431 (7006),* 350-355.

Apostolov, E. O., Basnakian, A. G., Ok, E. & Shah, S. V. (2012). Carbamylated low-density lipoprotein: nontraditional risk factor for cardiovascular events in patients with chronic kidney disease. *J Ren Nutr, 22 (1),* 134-138.

Apostolov, E. O., Ray, D., Savenka, A. V., Shah, S. V. & Basnakian, A. G. (2010). Chronic uremia stimulates LDL carbamylation and atherosclerosis. *J Am Soc Nephrol, 21 (11),* 1852-1857.

Apostolov, E. O., Shah, S. V., Ok, E. & Basnakian, A. G. (2005). Quantification of carbamylated LDL in human sera by a new sandwich ELISA. *Clin Chem, 51 (4),* 719-728.

Basnakian, A. G., Shah, S. V., Ok, E., Altunel, E. & Apostolov, E. O. (2010). Carbamylated LDL. *Adv Clin Chem, 51,* 25-52.

Bradford, M. M. (1976). A rapid and sensitive method for the quantitation of microgram quantities of protein utilizing the principle of protein-dye binding. *Anal Biochem, 72,* 248-254.

Brouillette, C. G., Anantharamaiah, G. M., Engler, J. A. & Borhani, D. W. (2001). Structural models of human apolipoprotein A-I: a critical analysis and review. *Biochim Biophys Acta, 1531 (1-2),* 4-46.

Bultel, S., Helin, L., Clavey, V., Chinetti-Gbaguidi, G., Rigamonti, E., Colin, M., Fruchart, J. C., Staels, B. & Lestavel, S. (2008). Liver X receptor activation induces the uptake of cholesteryl esters from high density lipoproteins in primary human macrophages. *Arterioscler Thromb Vasc Biol, 28 (12),* 2288-2295.

Chekulaeva, M. & Filipowicz, W. (2009). Mechanisms of miRNA-mediated post-transcriptional regulation in animal cells. *Curr Opin Cell Biol, 21 (3),* 452-460.

Chen, S. H., Yang, C. Y., Chen, P. F., Setzer, D., Tanimura, M., Li, W. H., Gotto, A. M., Jr. & Chan, L. (1986). The complete cDNA and amino acid sequence of human apolipoprotein B-100. *J Biol Chem, 261 (28),* 12918-12921.

Chen, X., Zhao, Y., Guo, Z., Zhou, L., Okoro, E. U. & Yang, H. (2011). Transcriptional regulation of ATP-binding cassette transporter A1 expression by a novel signaling pathway. *J Biol Chem, 286 (11),* 8917-8923.

Cuchel, M. & Rader, D. J. (2006). Macrophage reverse cholesterol transport: key to the regression of atherosclerosis? *Circulation, 113 (21),* 2548-2555.

Favari, E., Zanotti, I., Zimetti, F., Ronda, N., Bernini, F. & Rothblat, G. H. (2004). Probucol inhibits ABCA1-mediated cellular lipid efflux. *Arterioscler Thromb Vasc Biol, 24 (12),* 2345-2350.

Fielding, C. J. & Fielding, P. E. (1995). Molecular physiology of reverse cholesterol transport. *J Lipid Res, 36 (2),* 211-228.

Francis, G. A. & Perry, R. J. (1999). Targeting HDL-mediated cellular cholesterol efflux for the treatment and prevention of atherosclerosis. *Clin Chim Acta, 286 (1-2),* 219-230.

Gan, X., Kaplan, R., Menke, J. G., MacNaul, K., Chen, Y., Sparrow, C. P., Zhou, G., Wright, S. D. & Cai, T. Q. (2001). Dual mechanisms of ABCA1 regulation by geranylgeranyl pyrophosphate. *J Biol Chem, 276 (52),* 48702-48708.

Gelissen, I. C., Harris, M., Rye, K. A., Quinn, C., Brown, A. J., Kockx, M., Cartland, S., Packianathan, M., Kritharides, L. & Jessup, W. (2006). ABCA1 and ABCG1 synergize to mediate cholesterol export to apoA-I. *Arterioscler Thromb Vasc Biol, 26 (3),* 534-540.

Glass, C. K. & Witztum, J. L. (2001). Atherosclerosis. the road ahead. *Cell, 104 (4),* 503-516.

Goldstein, J. L. & Brown, M. S. (1977). The low-density lipoprotein pathway and its relation to atherosclerosis. *Annu Rev Biochem, 46,* 897-930.

Goldstein, J. L., DeBose-Boyd, R. A. & Brown, M. S. (2006). Protein sensors for membrane sterols. *Cell, 124 (1),* 35-46.

Goldstein, J. L., Ho, Y. K., Basu, S. K. & Brown, M. S. (1979). Binding site on macrophages that mediates uptake and degradation of acetylated low density lipoprotein, producing massive cholesterol deposition. *Proc Natl Acad Sci U S A, 76 (1),* 333-337.

Gonen, B., Goldberg, A. P., Harter, H. R. & Schonfeld, G. (1985). Abnormal cell-interactive properties of low-density lipoproteins isolated from patients with chronic renal failure. *Metabolism, 34 (1),* 10-14.

Goyal, T., Mitra, S., Khaidakov, M., Wang, X., Singla, S., Ding, Z., Liu, S. & Mehta, J. L. (2012). Current Concepts of the Role of Oxidized LDL Receptors in Atherosclerosis. *Curr Atheroscler Rep*.

Ha, T. Y. (2011a). MicroRNAs in Human Diseases: From Cancer to Cardiovascular Disease. *Immune Netw, 11 (3),* 135-154.

Ha, T. Y. (2011b). MicroRNAs in Human Diseases: From Lung, Liver and Kidney Diseases to Infectious Disease, Sickle Cell Disease and Endometrium Disease. *Immune Netw, 11 (6),* 309-323.

Himmelfarb, J., Stenvinkel, P., Ikizler, T. A. & Hakim, R. M. (2002). The elephant in uremia: oxidant stress as a unifying concept of cardiovascular disease in uremia. *Kidney Int, 62 (5),* 1524-1538.

Hirano, K., Yamashita, S., Nakagawa, Y., Ohya, T., Matsuura, F., Tsukamoto, K., Okamoto, Y., Matsuyama, A., Matsumoto, K., Miyagawa, J. & Matsuzawa, Y. (1999). Expression of human scavenger receptor class B type I in cultured human monocyte-derived macrophages and atherosclerotic lesions. *Circ Res, 85 (1),* 108-116.

Holzer, M., Gauster, M., Pfeifer, T., Wadsack, C., Fauler, G., Stiegler, P., Koefeler, H., Beubler, E., Schuligoi, R., Heinemann, A. & Marsche, G. (2011). Protein carbamylation renders high-density lipoprotein dysfunctional. *Antioxid Redox Signal, 14 (12),* 2337-2346.

Hörkkö, S., Huttunen, K., Kervinen, K. & Kesäniemi, Y. A. (1994). Decreased clearance of uraemic and mildly carbamylated low-density lipoprotein. *Eur J Clin Invest, 24 (2),* 105-113.

Hu, Y. W., Wang, Q., Ma, X., Li, X. X., Liu, X. H., Xiao, J., Liao, D. F., Xiang, J. & Tang, C. K. (2010). TGF-beta1 up-regulates expression of ABCA1, ABCG1 and SR-BI through liver X receptor alpha signaling pathway in THP-1 macrophage-derived foam cells. *J Atheroscler Thromb, 17 (5),* 493-502.

Incardona, J. P. & Eaton, S. (2000). Cholesterol in signal transduction. *Curr Opin Cell Biol, 12 (2),* 193-203.

Itabe, H. (2003). Oxidized low-density lipoproteins: what is understood and what remains to be clarified. *Biol Pharm Bull, 26 (1),* 1-9.

Jaisson, S., Pietrement, C. & Gillery, P. (2011). Carbamylation-derived products: bioactive compounds and potential biomarkers in chronic renal failure and atherosclerosis. *Clin Chem, 57 (11),* 1499-1505.

Kielar, D., Dietmaier, W., Langmann, T., Aslanidis, C., Probst, M., Naruszewicz, M. & Schmitz, G. (2001). Rapid quantification of human ABCA1 mRNA in various cell types and tissues by real-time reverse transcription-PCR. *Clin Chem, 47 (12),* 2089-2097.

Kraus, L. M. & Kraus, A. P., Jr. (2001). Carbamoylation of amino acids and proteins in uremia. *Kidney Int Suppl, 78,* S102-107.

Kunjathoor, V. V., Febbraio, M., Podrez, E. A., Moore, K. J., Andersson, L., Koehn, S., Rhee, J. S., Silverstein, R., Hoff, H. F. & Freeman, M. W. (2002). Scavenger receptors class A-I/II and CD36 are the principal receptors responsible for the uptake of modified low density lipoprotein leading to lipid loading in macrophages. *J Biol Chem, 277 (51),* 49982-49988.

Lam, M. C., Tan, K. C. & Lam, K. S. (2004). Glycoxidized low-density lipoprotein regulates the expression of scavenger receptors in THP-1 macrophages. *Atherosclerosis, 177 (2),* 313-320.

Langmann, T., Schumacher, C., Morham, S. G., Honer, C., Heimerl, S., Moehle, C. & Schmitz, G. (2003). ZNF202 is inversely regulated with its target genes ABCA1 and apoE during macrophage differentiation and foam cell formation. *J Lipid Res, 44 (5),* 968-977.

Libby, P., Ridker, P. M. & Hansson, G. K. (2011). Progress and challenges in translating the biology of atherosclerosis. *Nature, 473 (7347),* 317-325.

Malerod, L., Juvet, L. K., Hanssen-Bauer, A., Eskild, W. & Berg, T. (2002). Oxysterol-activated LXRalpha/RXR induces hSR-BI-promoter activity in hepatoma cells and preadipocytes. *Biochem Biophys Res Commun, 299 (5),* 916-923.

Maxfield, F. R. & van Meer, G. (2010). Cholesterol, the central lipid of mammalian cells. *Curr Opin Cell Biol, 22 (4),* 422-429.

Miller, Y. I., Choi, S. H., Fang, L. & Harkewicz, R. (2009). Toll-like receptor-4 and lipoprotein accumulation in macrophages. *Trends Cardiovasc Med, 19 (7),* 227-232.

Moore, K. J. & Freeman, M. W. (2006). Scavenger receptors in atherosclerosis: beyond lipid uptake. *Arterioscler Thromb Vasc Biol, 26 (8),* 1702-1711.

Moore, K. J., Rayner, K. J., Suarez, Y. & Fernandez-Hernando, C. (2010). microRNAs and cholesterol metabolism. *Trends Endocrinol Metab, 21 (12),* 699-706.

Moore, K. J. & Tabas, I. (2011). Macrophages in the pathogenesis of atherosclerosis. *Cell, 145 (3),* 341-355.

Moradi, H., Pahl, M. V., Elahimehr, R. & Vaziri, N. D. (2009a). Impaired antioxidant activity of high-density lipoprotein in chronic kidney disease. *Transl Res, 153 (2),* 77-85.

Moradi, H., Yuan, J., Ni, Z., Norris, K. & Vaziri, N. D. (2009b). Reverse cholesterol transport pathway in experimental chronic renal failure. *Am J Nephrol, 30 (2),* 147-154.

Murao, K., Terpstra, V., Green, S. R., Kondratenko, N., Steinberg, D. & Quehenberger, O. (1997). Characterization of CLA-1, a human homologue of rodent scavenger receptor BI, as a receptor for high density lipoprotein and apoptotic thymocytes. *J Biol Chem, 272 (28),* 17551-17557.

Navab, M., Berliner, J. A., Watson, A. D., Hama, S. Y., Territo, M. C., Lusis, A. J., Shih, D. M., Van Lenten, B. J., Frank, J. S., Demer, L. L., Edwards, P. A. & Fogelman, A. M. (1996). The Yin and Yang of oxidation in the development of the fatty streak. A review based on the 1994 George Lyman Duff Memorial Lecture. *Arterioscler Thromb Vasc Biol, 16 (7),* 831-842.

Ok, E., Basnakian, A. G., Apostolov, E. O., Barri, Y. M. & Shah, S. V. (2005). Carbamylated low-density lipoprotein induces death of endothelial cells: a link to atherosclerosis in patients with kidney disease. *Kidney Int, 68 (1),* 173-178.

Pello, O. M., Silvestre, C., De Pizzol, M. & Andres, V. (2011). A glimpse on the phenomenon of macrophage polarization during atherosclerosis. *Immunobiology, 216 (11),* 1172-1176.

Rader, D. J. & Pure, E. (2005). Lipoproteins, macrophage function, and atherosclerosis: beyond the foam cell? *Cell Metab, 1 (4),* 223-230.

Rayner, K. J., Suarez, Y., Davalos, A., Parathath, S., Fitzgerald, M. L., Tamehiro, N., Fisher, E. A., Moore, K. J. & Fernandez-Hernando, C. (2010). MiR-33 contributes to the regulation of cholesterol homeostasis. *Science, 328 (5985),* 1570-1573.

Ross, R. (1999). Atherosclerosis--an inflammatory disease. *N Engl J Med, 340 (2),* 115-126.

Sato, R. & Takano, T. (1995). Regulation of intracellular cholesterol metabolism. *Cell Struct Funct, 20 (6),* 421-427.

Schumaker, V. N. & Puppione, D. L. (1986). Sequential flotation ultracentrifugation. *Methods Enzymol, 128,* 155-170.

Schwartz, K., Lawn, R. M. & Wade, D. P. (2000). ABC1 gene expression and ApoA-I-mediated cholesterol efflux are regulated by LXR. *Biochem Biophys Res Commun, 274 (3),* 794-802.

Segrest, J. P., Jones, M. K., De Loof, H. & Dashti, N. (2001). Structure of apolipoprotein B-100 in low density lipoproteins. *J Lipid Res, 42 (9),* 1346-1367.

Stangl, H., Graf, G. A., Yu, L., Cao, G. & Wyne, K. (2002). Effect of estrogen on scavenger receptor BI expression in the rat. *J Endocrinol, 175 (3),* 663-672.

Steinberg, D. & Witztum, J. L. (2010). Oxidized low-density lipoprotein and atherosclerosis. *Arterioscler Thromb Vasc Biol, 30 (12),* 2311-2316.

Tall, A. R. (2008). Cholesterol efflux pathways and other potential mechanisms involved in the athero-protective effect of high density lipoproteins. *J Intern Med, 263 (3),* 256-273.

Thomas, M. J., Bhat, S. & Sorci-Thomas, M. G. (2008). Three-dimensional models of HDL apoA-I: implications for its assembly and function. *J Lipid Res, 49 (9),* 1875-1883.

Tontonoz, P. & Mangelsdorf, D. J. (2003). Liver X receptor signaling pathways in cardiovascular disease. *Mol Endocrinol, 17 (6),* 985-993.

Trepanier, D. J., Thibert, R. J., Draisey, T. F. & Caines, P. S. (1996). Carbamylation of erythrocyte membrane proteins: an in vitro and in vivo study. *Clin Biochem, 29 (4),* 347-355.

Tsuchiya, S., Kobayashi, Y., Goto, Y., Okumura, H., Nakae, S., Konno, T. & Tada, K. (1982). Induction of maturation in cultured human monocytic leukemia cells by a phorbol diester. *Cancer Res, 42 (4),* 1530-1536.

Tsuchiya, S., Yamabe, M., Yamaguchi, Y., Kobayashi, Y., Konno, T. & Tada, K. (1980). Establishment and characterization of a human acute monocytic leukemia cell line (THP-1). *Int J Cancer, 26 (2),* 171-176.

Valacchi, G., Sticozzi, C., Lim, Y. & Pecorelli, A. (2011). Scavenger receptor class B type I: a multifunctional receptor. *Ann N Y Acad Sci, 1229,* E1-7.

Vaziri, N. D. & Norris, K. (2011). Lipid disorders and their relevance to outcomes in chronic kidney disease. *Blood Purif, 31 (1-3),* 189-196.

Venkateswaran, A., Laffitte, B. A., Joseph, S. B., Mak, P. A., Wilpitz, D. C., Edwards, P. A. & Tontonoz, P. (2000). Control of cellular cholesterol efflux by the nuclear oxysterol receptor LXR alpha. *Proc Natl Acad Sci U S A, 97 (22),* 12097-12102.

Vickers, K. C., Palmisano, B. T., Shoucri, B. M., Shamburek, R. D. & Remaley, A. T. (2011). MicroRNAs are transported in plasma and delivered to recipient cells by high-density lipoproteins. *Nat Cell Biol, 13 (4),* 423-433.

Wang, N., Ranalletta, M., Matsuura, F., Peng, F. & Tall, A. R. (2006). LXR-induced redistribution of ABCG1 to plasma membrane in macrophages enhances cholesterol mass efflux to HDL. *Arterioscler Thromb Vasc Biol, 26 (6),* 1310-1316.

Wang, X., Collins, H. L., Ranalletta, M., Fuki, I. V., Billheimer, J. T., Rothblat, G. H., Tall, A. R. & Rader, D. J. (2007a). Macrophage ABCA1 and ABCG1, but not SR-BI, promote macrophage reverse cholesterol transport in vivo. *J Clin Invest, 117 (8),* 2216-2224.

Wang, Z., Nicholls, S. J., Rodriguez, E. R., Kummu, O., Horkko, S., Barnard, J., Reynolds, W. F., Topol, E. J., DiDonato, J. A. & Hazen, S. L. (2007b). Protein carbamylation links inflammation, smoking, uremia and atherogenesis. *Nat Med, 13 (10),* 1176-1184.

Watkins, H. & Farrall, M. (2006). Genetic susceptibility to coronary artery disease: from promise to progress. *Nat Rev Genet, 7 (3),* 163-173.

World Health Organization. (2008). *The Global Burden of Disease: 2004 Update*. WHO Library Cataloguing-in-Publication Data.

Yu, L., Cao, G., Repa, J. & Stangl, H. (2004). Sterol regulation of scavenger receptor class B type I in macrophages. *J Lipid Res, 45 (5),* 889-899.

Yvan-Charvet, L., Wang, N. & Tall, A. R. (2009). Role of HDL, ABCA1, and ABCG1 transporters in cholesterol efflux and immune responses. *Arterioscler Thromb Vasc Biol, 30 (2),* 139-143.

Zhao, Y., Pennings, M., Hildebrand, R. B., Ye, D., Calpe-Berdiel, L., Out, R., Kjerrulf, M., Hurt-Camejo, E., Groen, A. K., Hoekstra, M., Jessup, W., Chimini, G., Van Berkel, T. J. & Van Eck, M. (2010). Enhanced foam cell formation, atherosclerotic lesion development, and inflammation by combined deletion of ABCA1 and SR-BI in Bone marrow-derived cells in LDL receptor knockout mice on western-type diet. *Circ Res, 107 (12),* e20-31.

Zhu, Y., Liao, H., Xie, X., Yuan, Y., Lee, T. S., Wang, N., Wang, X., Shyy, J. Y. & Stemerman, M. B. (2005). Oxidized LDL downregulates ATP-binding cassette transporter-1 in human vascular endothelial cells via inhibiting liver X receptor (LXR). *Cardiovasc Res, 68 (3),* 425-432.

Zuo, Y., Yancey, P., Castro, I., Khan, W. N., Motojima, M., Ichikawa, I., Fogo, A. B., Linton, M. F., Fazio, S. & Kon, V. (2009). Renal dysfunction potentiates foam cell formation by repressing ABCA1. *Arterioscler Thromb Vasc Biol, 29 (9),* 1277-1282.

10 Supplementary Data

	CRF		ESRD on hemodialysis treatment	
	controls (*n*=17)	patients (*n*=17)	controls (*n*=14)	patients (*n*=14)
Clinical characteristics				
Gender (m/f)	(6/11)	(6/11)	(8/6)	(8/6)
Age (years)	34.9±9.3	34.6±8.6	36.0±9.6	36.7±10.2
BMI	22.3±2.5	22.7±3.5	24.0±3.1	25.3±4.8
KDOQI (3/4/5) (n)	-	6/8/3	-	-/-/14
Creatinine (mg/dl)	0.8±0.1	3.8±3.0***	0.9±0.2	7.7±4.1***
Serum lipids				
Cholesterol (mg/dl)	171.8±29.3	186.7±45.7	188.0±38.0	169.7±51.7
Triglycerides (mg/dl)	83.3±49.4	112.4±46.7	92.4±55.5	126.2±69.1
HDL (mg/dl)	49.5±15.9	42.0±12.9	53.2±14.1	36.8±9.3**
LDL (mg/dl)	105.6±31.9	122.3±41.2	116.3±32.8	107.7±47.6
Free Cholesterol (mg/dl)	50.2±8.2	55.7±13.3	54.4±11.2	53.4±18.1
Phospholipids (mg/dl)	216.1±26.9	210.9±40.1	229.6±35.9	213.1±65.2
Free fatty acids (mmol/l)	0.5±0.2	0.5±0.3	0.4±0.1	1.1±0.8**
Serum apoproteins				
Apo A-I (mg/dl)	155.4±27.9	145.1±32.0	166.6±29.8	132.4±27.0**
Apo A-II (mg/dl)	35.5±4.9	34.2±7.8	41.4±7.3	31.0±5.8***
Apo B (mg/dl)	71.3±22.5	88.0±26.4	76.6±27.1	68.1±18.4
Apo C-II (mg/dl)	2.9±1.5	3.8±1.6	3.2±1.5	4.5±2.9
Apo C-III (mg/dl)	7.6±2.5	11.2±7.1	11.1±4.4	17.7±11.0
Apo C-II/Apo C-III	0.4±0.2	0.4±0.2	0.3±0.1	0.3±0.1
Apo E (mg/dl)	7.9±1.6	8.9±1.9	8.9±2.8	14.1±14.1
Lp (a) (mg/dl)	10.2±9.5	29.4±31.3*	13.8±12.5	19.5±22.3

Table 15: Clinical characteristics, serum lipids and apoproteins of the study patients and controls (mean ± SD, * $p < 0.05$, ** $p < 0.01$, *** $p < 0001$, patients vs. controls

11 Curriculum Vitae

Personal Information

Name	Marianne HOLLAUS
Address	Linzer Straße 106c, 3100 St. Pölten, Austria
Phone, E-Mail	+43 660 6813804, mar.holl@gmx.at
Date and place of birth	2 April 1986, St. Pölten

Work Experience

08/2010 – 04/2012	practical training and master thesis Institute for Medical Chemistry, Medical University of Vienna, Währingerstraße 10, 1090 Wien Group: Ao. Univ. Prof. Dr. Witta Monika Strobl
06/2011 and 11/2011	student tutor of "Biochemische Übungen für Ernährungswissenschafter" University of Vienna, Dr.-Karl-Lueger-Ring 1, 1010 Wien
10/2011	student tutor of "Block 13 – Ernährung und Verdauung (Praktikum)" Medical University of Vienna, Spitalgasse 23, 1090 Wien
06/2009 – 07/2010 (temporarily)	marketing department: office assistant, promotion NÖ Pressehaus - Niederösterreichische Nachrichten (NÖN), Gutenbergstraße 12, 3100 St. Pölten
07/2008 – 02/2009	practical training and bachelor thesis Mental Health Research Institute of Victoria, Behavioural Neuroscience Laboratory, 30 Royal Parade, Parkville VIC 3052, Australia Group: Assoc. Prof. Maarten van den Buuse
10/2005 – 07/2006	administrative assistant Nimaro Arztmann GmbH, Am Platz 8-9, 9071 Köttmannsdorf

Education

since 10/2009	University of Vienna, master's programme "Molecular Biology"
2006 – 2009	University of Applied Sciences, IMC FH Krems, bachelor's programme "Medical and Pharmaceutical Biotechnology"
2000 – 2005	Handelsakademie (BHAK) St. Pölten, specialization "Information Technology and Information Management"

Publications

Chavez, C., **Hollaus, M**., Scarr, E., Pavey, G., Gogos, A., van den Buuse, M. (2010). The effect of estrogen on dopamine and serotonin receptor and transporter levels in the brain: An autoradiography study. *Brain Research* 1321, 51-59

Schreier, S.M., **Hollaus, M.**, Hermann, M., Jirovetz, L., Exner, M., Kapiotis, S., Gmeiner, B.M., Laggner, H. (accepted 2012). Carbamoylated free amino acids in uremia: HOCl generates volatile protein modifying and cytotoxic oxidant species from N-carbamoyl-threonine but not threonine. *Biochimie*